BIOLOGICAL REVIEWS
Cambridge Philosophical Society
Check for updates
Biol. Rev. (2024), pp. 000–000.
doi: 10.1111/brv.13116

Form and function of anguilliform swimming

Vincent Stin[1,2,*], Ramiro Godoy-Diana[1], Xavier Bonnet[3] and Anthony Herrel[2,4,5,6]

[1]*UMR 7636, PMMH, CNRS, ESPCI Paris-PSL, Sorbonne Université, Université Paris Cité, 7 Quai Saint-Bernard, Paris 75005, France*
[2]*Département Adaptation du Vivant, UMR 7179 MECADEV, MNHN/CNRS, 43 rue Buffon, Paris 75005, France*
[3]*UMR 7372 Centre d'Etude Biologique de Chizé, CNRS, 405 Route de Prissé la Charrière, Villiers-en-Bois 79360, France*
[4]*Department of Biology, Evolutionary Morphology of Vertebrates, Ghent University, K.L. Ledeganckstraat 35, Ghent 9000, Belgium*
[5]*Department of Biology, University of Antwerp, Universiteitsplein 1, Wilrijk 2610, Belgium*
[6]*Naturhistorisches Museum Bern, Bernastrasse 15, Bern 3005, Switzerland*

ABSTRACT

Anguilliform swimmers are long and narrow animals that propel themselves by undulating their bodies. Observations in nature and recent investigations suggest that anguilliform swimming is highly efficient. However, understanding the underlying reasons for the efficiency of this type of locomotion requires interdisciplinary studies spanning from biology to hydrodynamics. Regrettably, these different fields are rarely discussed together, which hinders our ability to understand the repeated evolution of this swimming mode in vertebrates. This review compiles the current knowledge of the anatomical features that drive anguilliform swimming, compares the resulting kinematics across a wide range of anguilliform swimmers, and describes the resulting hydrodynamic interactions using data from both *in vivo* experiments and computational studies.

Key words: anguilliform, locomotion, swimming, kinematics, hydrodynamics, adaptation, efficiency.

CONTENTS

* Author for correspondence (E-mail: vincent.stin@gmail.com).

I. INTRODUCTION

Anguilliform locomotion is one of the four main modes of swimming in fishes, together with the subcarangiform, carangiform, and thunniform modes (Breder, 1926; Lindsey, 1978). While animals using these different swimming modes can display similar kinematics (Di Santo *et al.*, 2021), anguilliform swimming can be described as an extreme mode of swimming as it is purely undulatory with little or no contribution of the fins. The whole surface of the body pushes against the water to generate propulsive forces, with at least one mechanical body wave being present and with a generally gradually increasing amplitude propagating backward along the body (Gray, 1933*a*; Lindsey, 1978).

The anguilliform swimming mode, named after the eel *Anguilla anguilla* (Breder, 1926), is the main swimming mode for a wide array of invertebrates and vertebrates. The body size of animals using this swimming mode spans from microscopic nematodes to several-metre-long snakes. Anguilliform swimming is effective in open water (marine or fresh water) and in more viscous media, such as thick mud or even sand (Nelson, Grande & Wilson, 1976; Ding *et al.*, 2012). The organisms that employ anguilliform swimming are elongated with a flexible body, and some feature highly reduced or no limbs or fins (Gans, 1975; Lindsey, 1978; Mehta *et al.*, 2010). Body elongation evolved independently in many lineages of fishes and in other vertebrates (Gans, 1975) with the most elongated organisms relying on anguilliform swimming (Ward & Mehta, 2010). Such convergence happened independently even within families; for example, it took place four times just within the catfish family Clariidae (Devaere *et al.*, 2007).

Recent work has challenged the concept of distinct swimming modes, previously classified as anguilliform, subcarangiform, carangiform, and thunniform (Bale *et al.*, 2015; Di Santo *et al.*, 2021; Akanyeti *et al.*, 2022). These authors suggested that these different patterns of swimming are not separate entities but rather converge and can be described by a unified model. They further highlight that two-dimensional (2D) kinematics may not be sufficient to differentiate these modes and that a full characterisation of the kinematics is needed. Interestingly, the least debated mode of locomotion is anguilliform swimming. Di Santo *et al.* (2021) differentiate anguilliforms on the basis of their smaller wavelength, while Akanyeti *et al.* (2022) base the differentiation on the larger number of segments needed.

Additional features of anguilliform swimmers include remarkable versatility and manoeuvrability, e.g. many species such as *Anguilla anguilla* can move on land (Gillis, 1998*a*). Their elongated body enables them to move through narrow, twisting crevices, to coil tightly and to knot, facilitating feeding in complex matrices (e.g. coral reefs) and offering a unique way to escape from predators (Herrel *et al.*, 2011*b*; Mehta *et al.*, 2010). Certain hagfishes, eels, and sea snakes can even perform backward swimming (D'Août & Aerts, 1999; Herrel *et al.*, 2011*a*; Islam *et al.*, 2006; Lim & Winegard, 2015). Many anguilliform swimmers can adjust their kinematics to shift between aquatic and terrestrial environments (Gillis, 1998*a*; Horner & Jayne, 2014; Pace & Gibb, 2011). Moreover, it has been shown that anguilliform-swimming eels display a high swimming efficiency (low energy expenditure relative to the distance travelled) and can swim long distances without feeding while consuming little body fat reserves (Van Ginneken *et al.*, 2005). Interestingly, most fish larvae have a tendency to use anguilliform swimming, even if they eventually adopt another swimming mode in line with their adult morphology (Lindsey, 1978).

The kinematics and dynamics of anguilliform swimming have been explored in laboratory settings in a variety of ray-finned and jawless fishes, notably eels (D'Août & Aerts, 1999; Gillis, 1998*a*; Gray, 1933*a*,*b*; Herrel *et al.*, 2011*a*; Matar, Candelier & Solliec, 2012; Müller *et al.*, 2001; Tytell, 2004*a*,*b*; Tytell & Lauder, 2004), gars (Long *et al.*, 1996; Webb, Hardy & Mehl, 1992), needlefishes (Kayan, Kozlov & Pyatetskii, 1978; Liao, 2002), catfish (Tack, Du Clos & Gemmell, 2021), ropefish (Pace & Gibb, 2011), lampreys (Du Clos *et al.*, 2019; Gemmell *et al.*, 2015*a*, 2016; McClellan *et al.*, 2016; Root *et al.*, 2010), and hagfish (Lim & Winegard, 2015; Long *et al.*, 2002). Importantly, anguilliform locomotion is not restricted to fish alone (Lighthill, 1969; Lindsey, 1978); it is also utilised by other aquatic animals like leeches (Chen, Friesen & Iwasaki, 2011; Jordan, 1998), salamanders (D'Aout & Aerts, 1999; D'Août, 1997; Gillis, 1997), and snakes (Graham *et al.*, 1987*b*; Jayne, 1985; Munk, 2008; Stin *et al.*, 2023).

The elongated body shape of anguilliform swimmers imposes specific hydrodynamic constraints, as both inertial and viscous interactions can play an important role (Tytell *et al.*, 2010*a*). Seminal models were developed for fishes several decades ago (Lighthill, 1960, 1971; Taylor, 1952; Wu, 1961, 1971). Later numerical models were able to take into account muscle activation (McMillen, Williams & Holmes, 2008; Tytell *et al.*, 2010*b*) and investigated the three-dimensional (3D) fluid–structure interactions generated by lateral undulations (Borazjani & Sotiropoulos, 2009; Kern & Koumoutsakos, 2006). These advanced models proposed ways to estimate optimal swimming behaviour and understand better the underlying mechanisms of anguilliform locomotion. In addition, physical models and robots that mimic anguilliform swimming have emerged as valuable tools for understanding locomotor mechanisms (Anastasiadis *et al.*, 2023; Thandiackal *et al.*, 2021). The field of biomimetic robots is making rapid progress, as shown by the many related studies (Gravish & Lauder, 2018; Li *et al.*, 2023; Salazar, Fuentes & Abdelkefi, 2018; Smits, 2019).

Fish locomotion has been the subject of several books (Hoar & Randall, 1978; Lighthill, 1975; Shadwick & Lauder, 2005; Taylor, Triantafyllou & Tropea, 2010; Videler, 1993) and recent reviews (Fish & Lauder, 2006; Gillis, 1996; Lauder, 2015; Liao, 2007; Sfakiotakis, Lane & Davies, 1999; Triantafyllou, Triantafyllou & Yue, 2000; Wu, 2011). However, anguilliform swimming is usually only briefly discussed. Furthermore, understanding the interactions between the swimmer's body, its kinematics, and its hydrodynamics, which form a complex feedback loop, necessitates an interdisciplinary review, currently lacking in the literature.

We are a long way from being able to understand how interactions between undulatory kinematics (e.g. frequency, amplitude, wave shape), external morphology, and internal anatomy optimise swimming efficiency. Models considering all these parameters and that could be applied to the morpho-functional diversity of elongated swimmers are only now emerging (Hoover *et al.*, 2021). Does a sea snake swim in the same way as a lamprey? How are the lateral undulations of an amphibious snake or eel altered when it transits between water and land? Such key questions remain unanswered, and the locomotor and morphological adaptations of anguilliform swimmers remain poorly understood.

This review aims to summarise and consolidate the current knowledge, from the anatomical intricacies of swimmers to the resulting hydrodynamic effects. The main objectives are: (*i*) to explain the structural features underlying anguilliform locomotion; (*ii*) to summarise the kinematic data available across species during routine swimming and in different contexts; (*iii*) to review the induced hydrodynamic mechanisms involved; and (*iv*) to discuss the implications for swimming efficiency.

II. ANATOMY OF ANGUILLIFORM SWIMMERS

(1) Musculotendinous system

The musculotendinous system is responsible for generating movement. It is therefore essential to understand how it works. During swimming, oscillatory movements are achieved through the coordinated activation of axial muscles, resulting in the characteristic lateral waves with progressively greater amplitude from front to back. The axial musculature comprises different types and groups of muscles with diverse but complementary functions (Gillis, 1998*b*).

In vertebrates, the muscles can broadly be categorised into two distinct functional groups; detailed descriptions can be found in Videler (1993) and Shadwick & Gemballa (2005). The first group of muscles is aerobic and is typically referred to as red muscle, arranged in bands along the body midline and mostly located just beneath the skin. The second type of muscles, the anaerobic white muscles, makes up the bulk of the muscle mass, and they are arranged in a complex 3D structure for high swimming proficiency over a wide range of speeds. Red muscles have been identified as mostly used for steady swimming (e.g. cruising), while white muscles are typically recruited for acceleration or for occasional swimming at a higher speed, e.g. sprinting (Coughlin, 2002; Gillis, 1998*b*). It is obvious that the phylogenetic and morpho-functional diversity associated with the diversity of anguilliform swimmers, ranging from teleost fishes to squamates, is also associated with diversity of musculotendinous systems (Danos, Fisch & Gemballa, 2008, Jayne, 1988*b*, 1985). Previous studies have shown that the muscles used to generate thrust vary considerably in their size, position, and function, both within a given species of fish and among different species of fishes (Altringham & Ellerby, 1999; Coughlin, 2002; Gemballa & Vogel, 2002; Gillis, 1998*b*; Wardle, Videler & Altringham, 1995; see Fig. 1). However, a comprehensive comparative anatomical study of the axial system across various anguilliform species is lacking to date.

During steady oscillatory swimming, muscles are activated in an antero-posterior travelling wave. The pattern of neural activity moves faster than the body curvature wave, causing variable phase differences between the two waves along the body, called neuromechanical phase lags (Tytell, Holmes & Cohen, 2011). The muscles have a dual function during swimming: as one side of the body is lengthened, the muscles generate force, resulting in both net positive mechanical

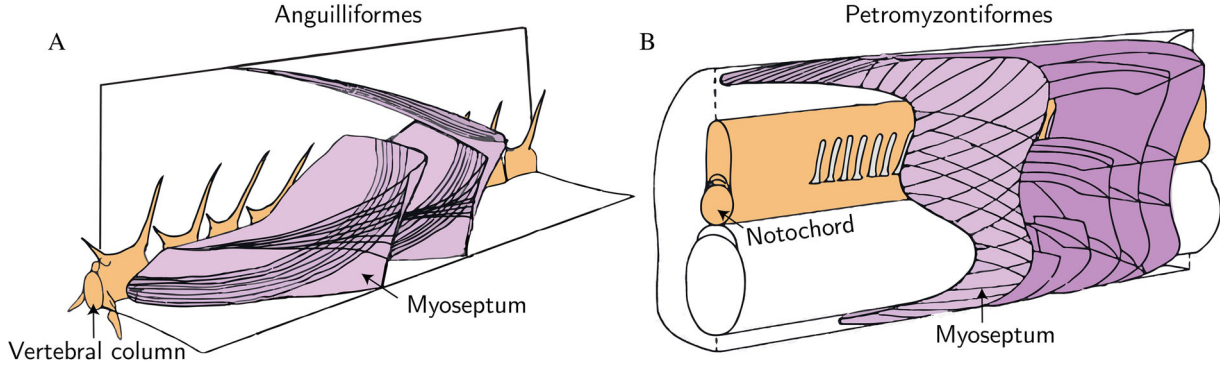

Fig. 1. Simplified representation of the myosepta of two orders of anguilliform swimmers: (A) Anguilliformes and (B) Petromyzontiformes. Modified after Gemballa & Vogel (2002). Orange colour highlights the vertebral column (A) *versus* notochord system (B). Further intra- and interspecific differences may arise in the number of vertebrae in other anguilliform swimmers. Purple colour highlights the muscle architecture. Many differences exist in the size and orientation of the muscle fibres.

work and increased body stiffness (Long, 1998). The phase lag is therefore crucial because the timing in which the muscle is activated during the swimming cycle will greatly influence swimming efficiency. The phase lag has been experimentally measured using electromyography (EMG) at different parts of the body in swimming eels (Gillis, 1998*a*; Grillner & Kashin, 1976; Wardle *et al.*, 1995), lamprey (McClellan *et al.*, 2016; Williams *et al.*, 1989), salamanders (Frolich & Biewener, 1992; Ryczko *et al.*, 2015) and snakes (Jayne, 1988*b*). Notably, anguilliforms exhibited a smaller phase lag compared to other types of swimmers.

One potential reason for this difference in fishes can be attributed to the musculotendinous systems of anguilliforms, which differ from those of carangiform and thunniform swimmers (Shadwick & Gemballa, 2005). Research on eels has emphasised that anguilliform swimmers possess shorter muscle segments and tendons, an anatomical configuration that may correspond to the localised transmission of force over short distances (Danos *et al.*, 2008). Additionally, studies on eels have shown a uniform distribution of muscle properties along their body, in contrast to other fishes (D'Août *et al.*, 2001). Some of these characteristics have also been observed in snakes with different ecological habits, with aquatic snakes tending to have shorter muscles and tendons (Jayne, 1988*b*, 1985; Mathou *et al.*, 2023).

The origin and function of the above-mentioned muscular properties were examined over 40 years ago (Blight, 1977). Mechanical tests showed that eels (Long, 1998) and lampreys (Tytell *et al.*, 2018) can increase their body stiffness by increasing muscle work to match the body's natural frequency to the driving frequency over a range of tail-beat frequencies. This could minimise the internal cost of bending the body during swimming.

Interestingly, one anatomical parameter that varies considerably among anguilliform swimmers is the total number of vertebrae, ranging from 100 to 400 in snakes (Gans, 1975) to none for leeches, lampreys, and hagfish. The total number of vertebrae can also vary between individuals of the same species, and studies have shown that individuals with significantly fewer vertebrae do not differ kinematically from individuals with more vertebrae [see Jayne (1985) for snakes, and Gillis (1997) for salamanders]. Muscles are not the sole contributors to the mechanical properties of swimming organisms as both the vertebral column and the skin can contribute substantially (Kenaley *et al.*, 2018; Nowroozi & Brainerd, 2014). For instance, in the case of the hagfish, the notochord plays a crucial role in adjusting the body's stiffness (Long *et al.*, 2002). By doing so, the notochord provides essential mechanical stability during steady swimming. For vertebrate anguilliform swimmers, the contribution of the vertebral column is still unclear as mechanical data are lacking, as emphasised by Nowroozi & Brainerd (2014).

The challenge posed by *in vivo* experiments triggered the development of a multitude of models to understand the interactions between the different parts of the body during swimming. Over time, this field of research has shifted, progressing from simpler rod models (Bowtell & Williams, 1991, 1994), reactive 'Lighthill' models (Pedley & Hill, 1999), and resistive 'Taylor' models (McMillen & Holmes, 2006; McMillen *et al.*, 2008) to models incorporating muscle mechanics (Bhalla, Griffith & Patankar, 2013; Cui & Zhang, 2023; Williams & McMillen, 2015). Advancements have led to the emergence of coupled reactive and resistive models (Chen *et al.*, 2011; Chen, Friesen & Iwasaki, 2012; Piñeirua, Godoy-Diana & Thiria, 2015; Piñeirua, Thiria & Godoy-Diana, 2017; Ramananarivo, Godoy-Diana & Thiria, 2013), sensory feedback models (Gazzola, Argentina & Mahadevan, 2015), 2D Navier–Stokes models incorporating muscle mechanics (Tytell *et al.*, 2010*b*), sensory feedback loops (Hamlet *et al.*, 2018), and even 3D Navier–Stokes models that encompass tendon mechanics (Ming *et al.*, 2019). The main findings of these models confirm the experimental observations that peak swimming speed and efficiency can be achieved by aligning body stiffness, tail-beat frequency, and muscle actuation. Different tail-beat frequencies are, however, possible for a given swimming speed based on muscle activation strength. The models showed an optimal ratio of the bending to muscle activation wave, matching the experimentally observed phase lags.

A particularity of many anguilliform swimmers is that they can move both in water and on land. EMG studies on eels (Gillis, 1998*a*) and lungfish (Horner & Jayne, 2008, 2014) found that there was no phase lag during terrestrial locomotion, suggesting that the increased viscosity of water relative to air increased the phase lag. This highlights the different ways in which activation of the musculo-skeletal system is optimised to function in these two very different environments. However, the presence of a neuromechanical phase lag seems to be inherent to undulatory locomotion, especially when distributed forces such as resistive or inertial forces significantly influence the movement (Ding *et al.*, 2013).

Another particularity of anguilliform swimmers is their ability to perform backward swimming. Studies on backward-swimming eels have shown that, compared to forward swimming, they exhibit a significantly higher midline flexion of the body, resulting in increased strain along the body (D'Août & Aerts, 1999; Long, Shepherd & Root, 1997). Further research on backward-swimming lamprey revealed the absence of a stable spatial body orientation during this maneuver (Islam *et al.*, 2006). These findings indicate that backward swimming comes with a cost, and is probably accompanied by reduced swimming efficiency.

(2) External morphology

The shape of a fish's body can be a good indicator of its locomotor specialisation (Feilich, 2016; Webb, 1984, Di Santo *et al.*, 2021), although this parameter alone may not be sufficient to differentiate fully between swimming behaviours (Satterfield, Claverie & Wainwright, 2023). Nevertheless, one of the main characteristics shared by all anguilliform swimmers is their low body length (L) to height (H) aspect ratio, or fineness ratio (AR = L/H). This particular parameter serves as a reliable means to distinguish the morphology of

anguilliform swimmers from that of other types of oscillatory swimmers. Anguilliform swimmers typically exhibit an AR that is 3–5 times smaller compared to other types of swimmers (Van Weerden, Reid & Hemelrijk, 2014). Yet, despite sharing a simplified elongated body form, anguilliform swimmers exhibit strong variation in internal structure as well as external shape across species (Figs 1–3 and Table 1).

While their streamlined bodies maintain a consistent form, disparities arise in terms of the presence and dimensions of the fins. For example, eels and lampreys possess median fins (Fig. 2), which augment the lateral surface area, facilitating more efficient transmission of fish's momentum to the water. Eels, needlefish, and ropefish also employ pectoral fins to enhance maneuverability during slow swimming (Gillis, 1998*a*; Liao, 2002; Pace & Gibb, 2011). However, snakes and hagfish do not possess fins, highlighting that fins are not essential for anguilliform locomotion. Sea snakes evolved specialised paddle-like tails, increasing the surface of contact with the water (Aubret & Shine, 2008; Brischoux *et al.*, 2010). Sea kraits (Laticaudinae), a lineage of sea snake, and semi-aquatic snakes exhibit remarkable adaptability to moving both on land and in the water. They have the ability to deploy a ventral keel when swimming through the modification of their trunk cross section through rib movements and can retract the ribs to move on land (Brischoux *et al.*, 2010), a feature shared with other highly aquatic snakes such as *Acrochordus* (A. Herrel, personal observations). By controlling their body shape in this way, water snakes (*Nerodia sipedon*) partially resemble sea kraits that are permanently laterally flattened (Pattishall & Cundall, 2008). Hydrodynamic constraints also shape the head of anguilliform swimmers; for instance snakes that feed on aquatic prey tend to exhibit relatively narrow head shapes (Segall *et al.*, 2016).

Three-dimensional computational fluid dynamics studies (Borazjani & Sotiropoulos, 2010; Van Rees, Gazzola & Koumoutsakos, 2013, 2015), muscle interaction models (Tokíc & Yue, 2012) as well as reactive models (Eloy, 2013) found that swimming performance, given anguilliform kinematics, is highly dependent on the external morphology of the swimmer. These models suggest that caudal fins are efficient attributes for anguilliform swimming, but result in a trade-off between swimming speed and efficiency, which together with historical and environmental constraints may explain the differences in the shapes and sizes of anguilliform

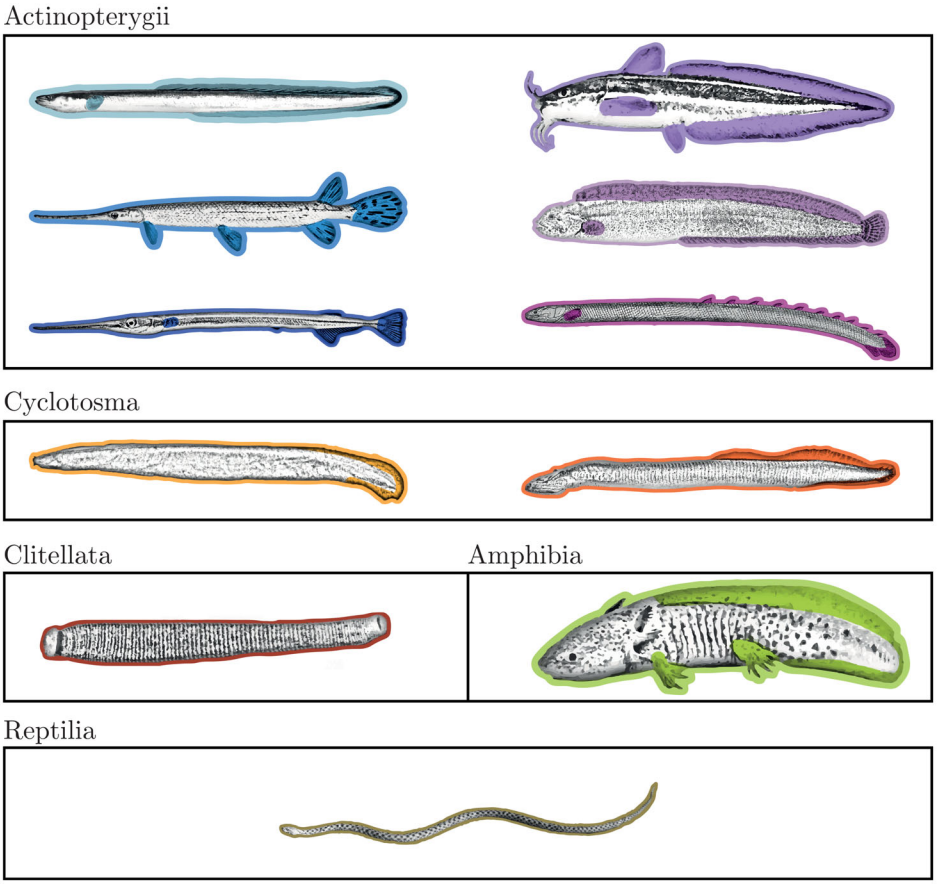

Fig. 2. Diversity of morphology among anguilliform swimmers. Images sorted by class and scaled to the same size. Fins and/or limbs are highlighted. Actinopterygii, from top left to bottom right: *Anguilla anguilla* (eel), *Plotosus lineatus* (catfish), *Lepisosteus osseus* (gar), *Pholis laeta* (gunnel), *Strongylura marina* (needlefish), *Erpetoichthys calabaricus* (ropefish); Cyclostoma: *Eptatretus stoutii* (hagfish), *Petromyzon marinus* (lamprey); Clitellata: *Hirudo verbana* (leech); Amphibia: *Ambystoma mexicanum* (axolotl); Reptilia: *Natrix tessellata* (dice snake).

Fig. 3. Diversity of wetted surfaces. (A) Scaleless body of the sea lamprey (*Petromyzon marinus* with seven gill pores located on the side of the head. The rest of the body is very smooth. Photograph from Jacobs & O'Donnell (2009). (B) Ganoid scales of the longnose gar (*Lepisosteus osseus*, photograph: G. Burgess). (C) Oval scales of the aquatic dice snake (*Natrix tessellata*, photograph: F. Crovetto).

swimmers found in nature (Tokíc & Yue, 2012). Computations suggest that without fins, elongate swimmers can still achieve high swimming efficiency (Van Rees *et al.*, 2013). Body size decorrelation also shows that for a given length, the width of the body has the largest influence on performance: a thin shape maximises the forward velocity whereas

Table 1. Morphological features of swimmers in investigations of anguilliform swimming. Species with typically small, embedded scales are considered scaleless. References: 1, D'Août & Aerts (1999); 2, Müller *et al.* (2001); 3, Matar *et al.* (2012); 4, Gillis (1998*a*); 5, Tytell & Lauder (2004); 6, Tytell (2004*b*); 7, Tytell (2004*a*); 8, Herrel *et al.* (2011*a*); 9, Webb *et al.* (1992); 10, Long *et al.* (1996); 11, Kayan *et al.* (1978); 12, Liao (2002); 13, Tack *et al.* (2021); 14, Donatelli *et al.* (2017); 15, Videler (1993); 16, Pace & Gibb (2011); 17, Lim & Winegard (2015); 18, Long *et al.* (2002); 19, Root *et al.* (2010); 20, Gemmell *et al.* (2015*a*); 21, Gemmell *et al.* (2016); 22, McClellan *et al.* (2016); 23, Lehn (2019); 24, Du Clos *et al.* (2019); 25, Jordan (1998); 26, Chen *et al.* (2011); 27, Chen *et al.* (2012); 28, Gillis (1997); 29, D'Août (1997); 30, D'Aout & Aerts (1999); 31, Graham *et al.* (1987*b*); 32, Munk (2008); 33, Jayne (1985); 34, Stin *et al.* (2023).

Order	Species	Body length (cm)	Vertebrae present	Scales present	References
Hirudiniformes	*Hirudo medicinalis*	2–11	No	No	25
	Hirudo verbana	9–13	No	No	26, 27
Petromyzontiformes	*Petromyzon marinus*	7–54	No	No	19, 20, 21, 22, 23, 24
Myxiniformes	*Eptatretus stoutii*	26–30	No	No	17
	Myxine glutinosa	26–31	No	No	17, 18
Polypteriformes	*Erpetoichthys calabaricus*	23.6	Yes	Yes	16
Lepisosteiformes	*Lepisosteus osseus*	46–76	Yes	Yes	9, 10
Anguilliformes	*Pisodonophis boro*	17–22	Yes	No	8
	Heteroconger hassi	23–27	Yes	No	8
	Anguilla anguilla	10–30	Yes	No	1, 2, 3
	Anguilla rostrata	8–39	Yes	No	4, 5, 6, 7
Siluriformes	*Plotosus lineatus*	7.4	Yes	No	13
Beloniformes	*Belone belone*	40–48	Yes	Yes	11
	Strongylura marina	23.3	Yes	Yes	12
Perciformes	*Lumpenus sagitta*	18–23	Yes	No	14
	Xiphister mucosus	19–20	Yes	Yes	14
	Anoplarchus insignis	12	Yes	No	14
	Pholis laeta	16–18	Yes	Yes	14
	Apodichthys flavidus	16–23	Yes	No	14
	Ronquilus jordani	14–18	Yes	Yes	14
	Ammodytes marinus	9–11	Yes	Yes	15
	Hyperoplus lanceolatus	29–33	Yes	Yes	14, 15
Caudata	*Siren intermedia*	34–38	Yes	No	28
	Ambystoma mexicanum	1–23	Yes	No	29, 30
Squamata	*Hydrophis platurus*	45–70	Yes	Yes	31
	Thamnophis sirtalis	13–21	Yes	Yes	32
	Nerodia fasciata	22–71	Yes	Yes	33
	Elaphe guttata	33–142	Yes	Yes	33
	Natrix tessellata	65–84	Yes	Yes	34

a more stocky body is beneficial for efficiency (Van Rees *et al.*, 2015).

(3) Skin properties

Another important variable is the nature of the wetted surface. The outer layer of the swimmer is often a complex 3D structure of epidermis, scales and/or mucus that have roles including physical protection, prevention of surface fouling, and the modification of flow during swimming. When present, scales can vary in shape, structure, and size among species (Fig. 3) but also along the body of the swimmer. For a detailed review on the different types of skin and their functions, see Akat *et al.*, (2022). In aquatic animals, the skin has a dual function of participating in internal mechanics and interacting with the surrounding water.

Mechanical studies on the skin of the longnose gar (*Lepisosteus osseus*) showed that the removal of caudal scales reduced both body flexural stiffness and swimming speed (Long *et al.*, 1996). Studies on different snake species found significant interspecific variation in skin mechanical properties, as well as a dependence on the location of scales on the snake, and it is generally assumed that generalist species have more homogeneous skin characteristics along the body (Jayne, 1988*a*). Studies of hagfish, which have loose-fitting skin, also revealed strong interspecific variations in skin stiffness with body size, but also in its isotropic properties (Clark *et al.*, 2016; Kennedy *et al.*, 2021). Hagfish of the genus *Eptatretus* have an anisotropic skin, i.e. the skin is stiffer in the longitudinal axis, a property shared with eels (Hebrank, 1980) and possibly snakes (Jayne, 1988*a*). By contrast, the skin in *Myxine* hagfish is isotropic and less flexible. The interspecific variation in hagfish skin is closely related to both their phylogeny and knotting ability. These results suggest that the skin participates in force transmission while resisting torsion due to its anisotropic properties. This is, however, not the case for all anguilliform swimmers, perhaps because of phylogenetic constraints. Nevertheless, these species seem to compensate through other structures, like the notochord in hagfish which plays an important role in maintaining body stiffness (Long *et al.*, 2002). Using a large sample of actinopterygian fishes, Kenaley *et al.*, (2018) found that a skin stiffness had an influence on the propulsive wavelength, supporting the hypothesis that the skin plays an important role in force transmission.

Anguilliform swimmers such as eels and lampreys often have reduced or no scales, whereas elongated bony fishes more typically have scales. The external structure of the skin, particularly the scales, can affect the surrounding flow of the swimmer and may reduce the drag. There has been particularly extensive research on this issue on sharks for more than 30 years (Dean & Bhushan, 2010). Non-smooth surfaces and their effect on drag have also been studied using simplified geometries, known as riblets, as well as fish skin, and bio-inspired scales (Lauder *et al.*, 2016; Liu *et al.*, 2020). In recent research, the use of 3D printed shark skin foils has focused attention on the influence of scale pattern and spacing on drag (Wen *et al.*, 2015), and the impact of denticle size (Domel *et al.*, 2018). Overall, these studies propose that the 3D geometry and pattern of scales play a crucial role in stabilising the laminar boundary layer, effectively avoiding flow separation and minimising skin friction drag. However, it is essential to acknowledge that we are still far from achieving a complete replication of the intricate swimming conditions that encompass the swimmer's complex geometry and flexibility.

Another complication is that many fish secrete mucus. Histological studies have shown that there is no obligatory correlation between the 3D structure of the scales and their appearance when covered by mucus, which makes it extremely difficult to anticipate its hydrodynamic effects (Wainwright & Lauder, 2017). As first suggested by Breder (1926) and reviewed by Shepard (1968), this mucus has been hypothesised to, among many other functions, optimise the hydrodynamic properties of the fish. Recent work measured the effect of mucus secretion of loaches (*Misgurnus anguillicaudatus*) and found a strong influence on the reduction of skin friction drag (Seo *et al.*, 2020).

There have been only a limited number of in vivo measurements on the boundary layer flow of swimming fish (Anderson, Mcgillis & Grosenbaugh, 2001; Yanase & Saarenrinne, 2015), which underscores the complexity of such experiments. Similarly, numerical simulations in this area have been relatively scarce. Some studies have digitised and simulated a few shark scales in boundary layer flows (Boomsma & Sotiropoulos, 2016; Miyazaki *et al.*, 2018), while others have estimated skin friction based on simplified, rigid geometries without considering the influence of scales (Ehrenstein & Eloy, 2013). This demonstrates the significant computational challenges involved in incorporating the effects of skin friction in 3D models of swimmers, a task that, to the best of our knowledge, remains unaccomplished to date.

The impact of the topology of the wetted surface and potential drag reduction is currently a subject of extensive research. For anguilliform swimmers, which range from snakes with diverse scale patterns to lampreys with smoother mucous-covered skin, the influence of these surface variations on swimming drag remains virtually unknown.

III. SWIMMING KINEMATICS

The way anguilliform swimmers move through water is directly influenced by complex interactions between anatomical structures during the continuous body deformations. Accurate measurements of how their bodies move are crucial for both biologists and engineers studying how they swim. These measurements serve two main purposes. Firstly, they aim to understand the basic aspects of how different species move in different contexts. Secondly, they provide important information to create and validate models used to study the behaviour of the fluid around these swimming organisms.

(1) Experimental methods

Since pioneering studies on eels, anguilliform swimming kinematics have been studied in various species, traditionally under artificial conditions using swimming tanks under laboratory conditions (Gray, 1933*a*,*b*). These tanks can be categorised into two types: still water tanks and recirculating flumes. The former are employed to observe voluntary swimming and are better suited for studying a fish's normal behaviour (e.g. Long *et al.*, 2002). The latter type is designed for controlled steady-swimming studies, providing a convenient means to regulate swimming speed (e.g. Gillis, 1997). Recent studies introduced turbulence-inducing tanks for more complex behavioural studies (Liao, 2007). However, the effect of turbulence on kinematics has not been reported for anguilliform swimmers.

The vast majority of studies of anguilliform swimming have involved 2D measurements, usually filming the oscillations in the horizontal plane either from above or below. This non-invasive method allows for unrestrained swimming trials. The kinematics are then derived by processing the footage and monitoring the coordinates of several points along the mid-line of the swimmer, connected by segments. The time variation of the mid-line points allows calculation of kinematic parameters such as the frequency (f), amplitude (A), wavelength (λ) and speed (V) of the mechanical wave travelling along the body of the swimmer, swimming at speed U (Fig. 4). Most studies have focused on steady swimming, defining it as swimming in a straight line at constant speed (D'Août, 1997), sometimes defining it as involving a small change in centre of mass velocity over a tail-beat cycle (Munk, 2008).

(2) General kinematic parameters

(a) *Swimming frequency*

The relationship between the tail-beat frequency (f) and swimming speed (U) is frequently reported in the literature (Fig. 5). The strong positive relationship between U and f observed in various fishes (Bainbridge, 1958) was supported by a meta-analysis on undulatory swimmers (Van Weerden *et al.*, 2014). Wave frequency typically increases linearly with swimming speed, but the slope varies among taxa.

Variation of wave frequency along the body is rarely mentioned, but has been reported to increase along the body for ropefish (Pace & Gibb, 2011). Frequency variation along the body occurs when the body wave is more complex, comprising a superposition of several waves. The body kinematics can therefore be decomposed into harmonics (Root *et al.*, 2010).

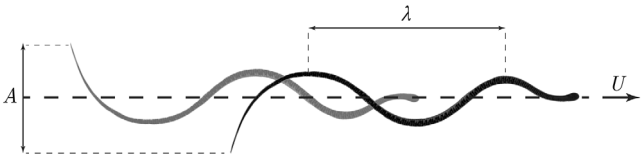

Fig. 4. Illustration of the main kinematic parameters in anguilliform swimming. Forward velocity U is distinguished by a mechanical wave travelling in the rearward direction at speed V and wavelength λ, with peak-to-peak amplitude at the tail A, and a tail-beat frequency f.

(b) *Body wave speed*

A strong positive correlation was found between body wave speed, V, and U (Van Weerden *et al.*, 2014) (Fig. 6). V typically increases linearly with U and its value is often given as a ratio U/V called slip, which is linked to propeller efficiency (Webb, 1971). During steady swimming, the travelling wave is faster than U, making the slip value lower than 1 (Videler, 1993).

V can be measured by estimating the time between the peaks in the lateral excursion of the mid-line of the swimmer (Tytell & Lauder, 2004). V is sometimes estimated using the relation $V = \lambda f$ (Webb, Kostecki & Stevens, 1984). Although this is a reasonable approximation, it is essential to acknowledge that the local behaviour of the body may not follow a linear pattern. Although V has been reported to be constant along the body of *Anguilla anguilla* (Gillis, 1998*a*), this is not always the case. Indeed, V increases along the body at high speeds for snakes (Graham *et al.*, 1987*b*; Munk, 2008) and salamanders (Gillis, 1997), decreases at high speeds for needlefish (Liao, 2002), and is locally variable in hagfish (Lim & Winegard, 2015), but the mean speed across the body is independent of U.

(c) *Body wavelength*

Anguilliform swimmers undulate their bodies at wavelengths (λ) shorter than their body length (L). Over the range of speeds and species studied, λ is generally between $0.5L$ and $1L$ (Fig. 7). By contrast, λ is either equal to or larger than L for subcarangiform and carangiform swimmers (Webb, 1975). λ is usually measured as the distance between two successive peaks on the body mid-line.

Changes in λ with speed differ across taxa of anguilliform swimmers. It increases with swimming speed in eels (Gillis, 1998*a*) and in needlefish (Liao, 2002), decreases with swimming speed for hagfish (Lim & Winegard, 2015) and the snake *Nerodia pictiventris* (Jayne, 1985) and does not change significantly with swimming speed for salamanders (Gillis, 1997), burrowing eels (Herrel *et al.*, 2011*a*), lampreys (McClellan *et al.*, 2016) or the snake *Pelamis platurus* (Graham *et al.*, 1987*b*).

λ can also be position dependent, as it has been reported to increase along the body for snakes (Graham *et al.*, 1987*b*; Jayne, 1985; Munk, 2008) and ropefish (Pace & Gibb, 2011), decrease along the body for eels (Müller *et al.*, 2001), lampreys (Root *et al.*, 2010) and longnose gars (Long *et al.*, 1996), and to vary along the body for hagfish (Lim & Winegard, 2015).

Recent numerical investigations found that anguilliform kinematics outperformed carangiform ones when swimming at $\lambda < L$ and *vice versa* when swimming at $\lambda > L$ (Khalid *et al.*, 2020, 2021). Moreover, anguilliform swimmers can improve the pressure component of the axial force by using greater λs, but this increases frictional drag on the

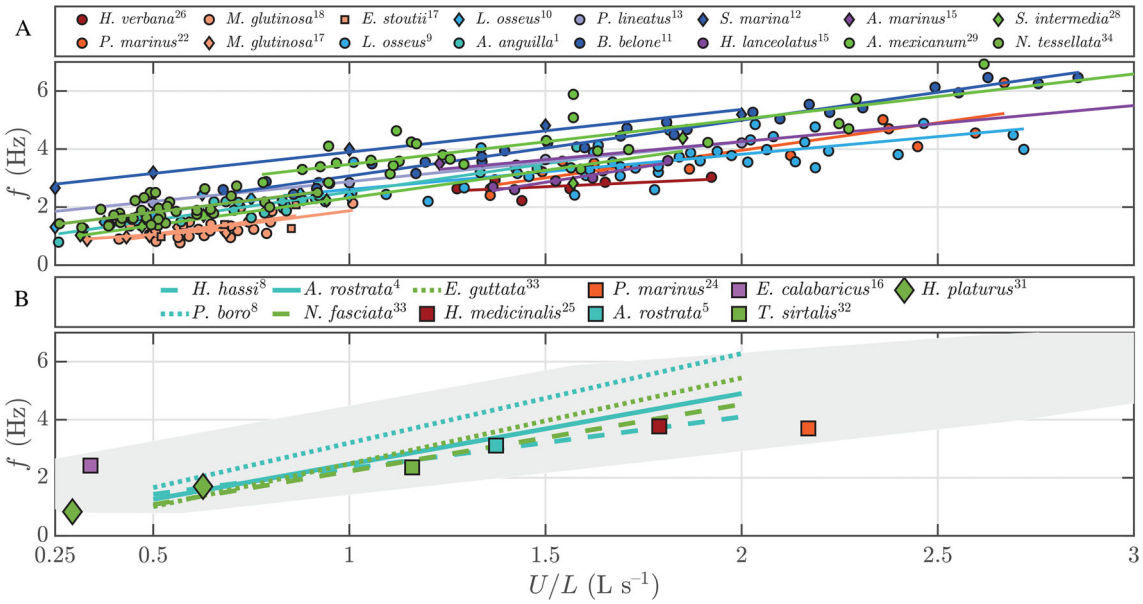

Fig. 5. Relationship between tail-beat frequency (f) and length-specific swimming speed (U) across anguilliform swimmers. (A) Compilation of data from published studies. Each colour represents an order of swimmers, as compiled in Table 1. Different symbols represent either different species and/or studies. A separate linear regression is plotted for each data set. (B) Results from studies where only regression equations (lines) or mean values (symbols) were available. The grey shaded region represents the surface covered by the data points in A. L = body length. Superscript numbers indicate references listed in the footnote to Table 1.

swimmer's body, negating the advantage by requiring greater power from the muscles. This observation was supported by foil simulations conducted by Chao, Alam & Cheng (2022). Khalid *et al.* (2021) suggested that anguilliform swimmers may find it challenging to swim with higher undulatory λs due to their body shape and physical characteristics. Conversely, lower λ leads to a more consistent thrust (Chao *et al.*, 2022). However, in situations where rapid escape manoeuvres are required, higher λ may enable greater speed and agility (Khalid *et al.*, 2021; Chao *et al.*, 2022).

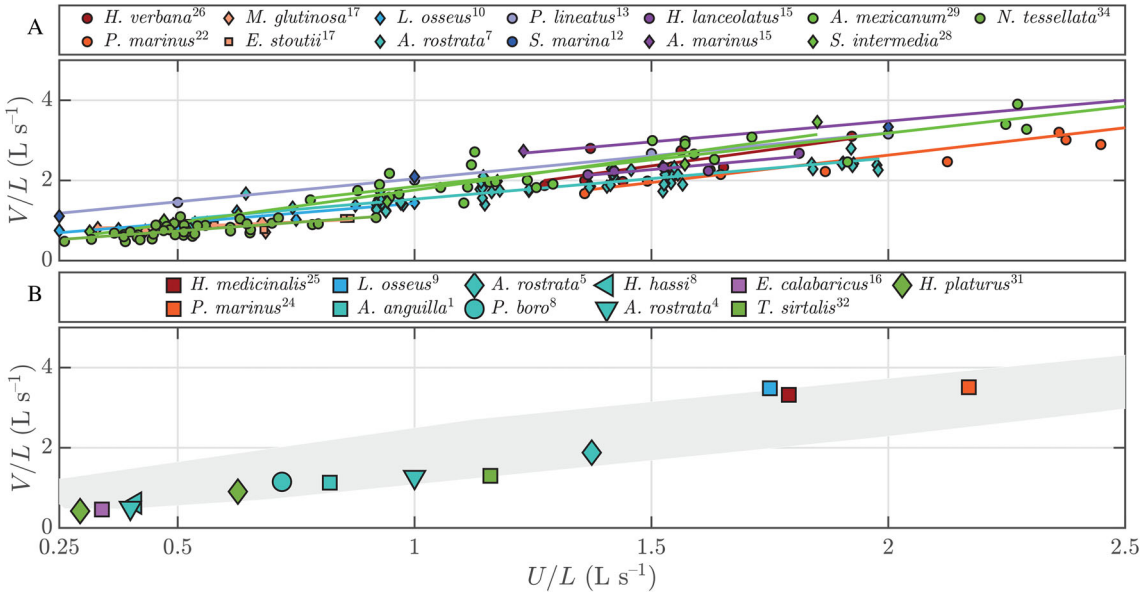

Fig. 6. Relationship between body deformation wave speed (V) and swimming speed (U) across anguilliform swimmers. (A) Compilation of data from published studies. Each colour represents an order of swimmers, as compiled in Table 1. Different symbols represent either different species and/or studies. A separate linear regression line is plotted for each data set. (B) Results from studies where only mean values were available. The grey shaded region represents the surface covered by the data points in A. L = body length. Superscript numbers indicate references listed in the footnote to Table 1.

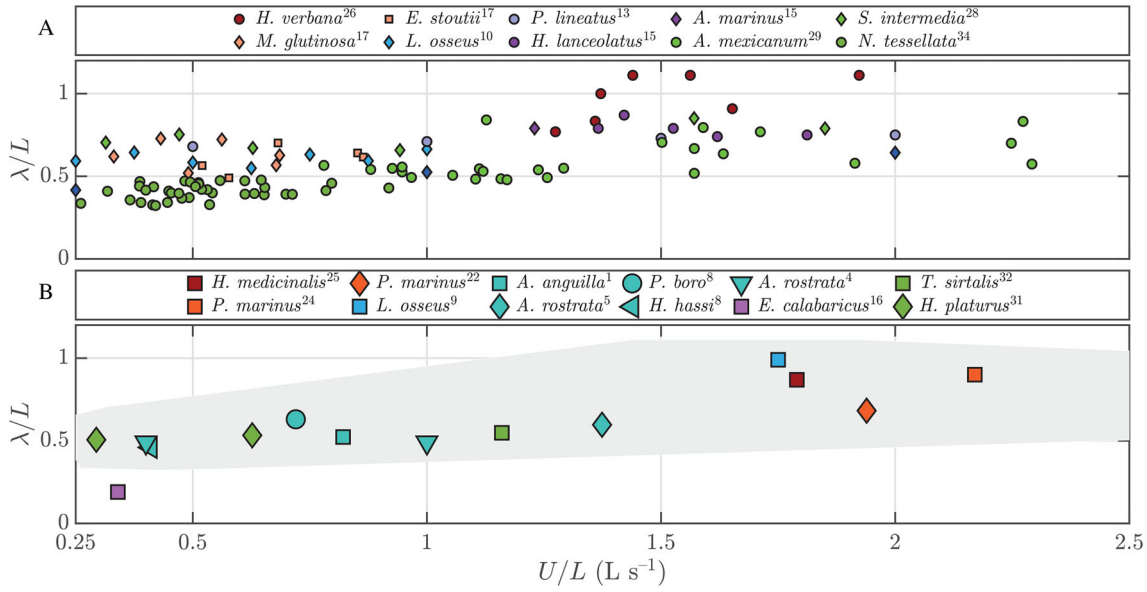

Fig. 7. Relationship between swimming wavelength (λ) and swimming speed (U) across anguilliform swimmers. (A) Compilation of data from published studies. Each colour represents an order of swimmers, as compiled in Table 1. Different symbols represent either different species and/or studies. (B) Results from studies where only mean values were available. The grey shaded region represents the surface covered by the data points in A. L = body length. Superscript numbers indicate references listed in the footnote to Table 1.

(*d*) *Body amplitude*

Concerning the lateral deflection of the body, the parameter mostly reported is the tail-beat amplitude (TBA). The definition of TBA differs among studies and can either be the amplitude of the body wave (A) or the distance between the points of maximum tail excursion. Using the second definition, TBA is around 5–20% of L across anguilliform swimmers (Fig. 8). TBA is often weakly or not correlated to U, and can show opposing relationships between closely related species (Lim & Winegard, 2015). Li

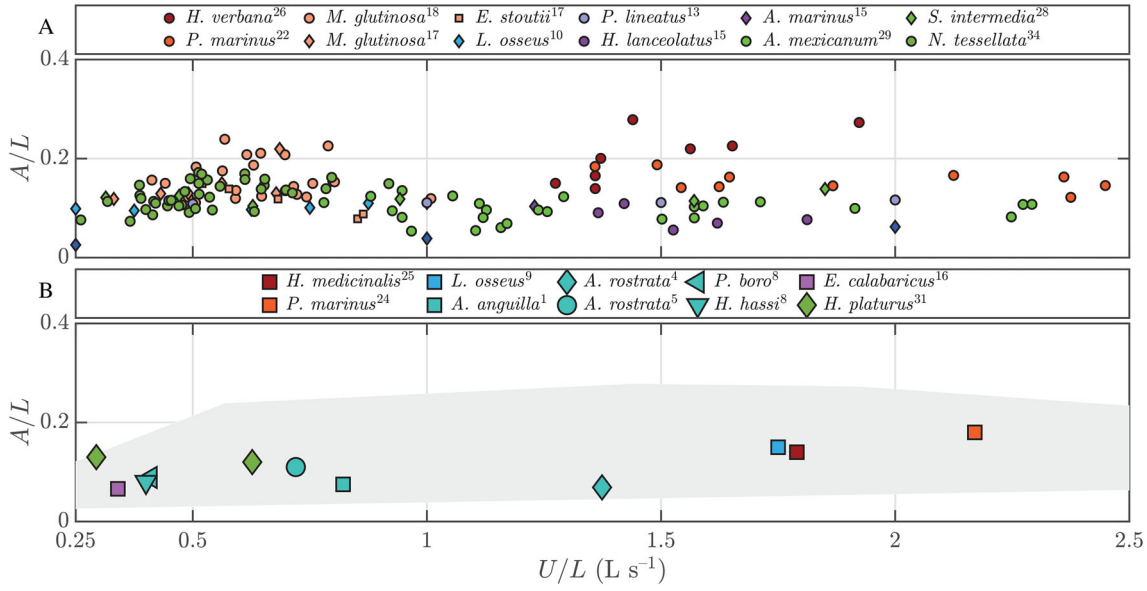

Fig. 8. Relationship between tail-beat amplitude (A) and swimming speed (U) across anguilliform swimmers. (A) Compilation of data from published studies. Each colour represents an order of swimmers, as compiled in Table 1. Different symbols represent either different species and/or studies. (B) Results from studies where only mean values were available. The grey shaded region represents the surface covered by the data points in A. L = body length. Superscript numbers indicate references listed in the footnote to Table 1.

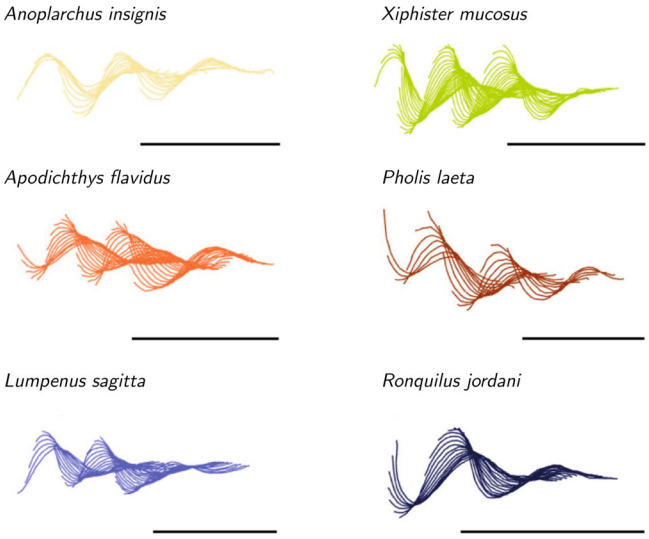

Fig. 9. Evolution of tail-beat amplitude along the body with time for different anguilliform species. The horizontal bar shows one body length and the different lines show the mid-line trace over two tail-beats. Note that different species employ recruitment of the body into lateral oscillations at more or less anterior positions along the body. Adapted from Donatelli *et al.* (2017).

et al. (2021) emphasised the importance of maintaining a narrow range of TBA while adjusting f to control speed.

The amplitude profile along the body can vary with U and differs among species (Fig. 9). At low speeds, anguilliform swimmers primarily utilise the posterior part of their body (D'Août & Aerts, 1999; Gillis, 1997), resulting in an exponential shape of the amplitude profile from head to tail. As U gradually increases, the contribution of the anterior part of the body becomes more significant, while the TBA remains relatively unchanged. This is likely due to morphological constraints, but this remains poorly explored. Tytell (2004*b*) derived an expression of the evolution of the lateral excursion along the body of an anguilliform swimmer as:

$$y(s,t) = Ae^{\alpha(s-1)} \sin\left(\frac{2\pi}{\lambda}[s - Vt]\right), \quad (1)$$

where s is the distance along the body, t is time and α is the growth parameter.

This model characterises well the amplitude along the body of an eel at relatively low speed, and that of needlefish, where the exponential amplitude profile remains consistent across a wide range of U due to its multiple caudal fins (Liao, 2002). The growth parameter α is used to describe the variation of the amplitude along the body of a swimmer. However, it may not be universally applicable as there are variations in the general pattern of body amplitude among different swimmers (Fig. 9).

For certain species like hagfish (Lim & Winegard, 2015) and salamanders at high speeds (Gillis, 1997), the head plays a significant role, resulting in minimal amplitude being observed just posterior to the head, followed by a linear increase along the body. In lampreys swimming at high speeds, the amplitude also increases linearly, but peak amplitude occurs before the tail tip and then decreases considerably (Gemmell *et al.*, 2016). Moreover, this model assumes that f is constant along the body, which is not always the case.

An alternative approach proposed by Tack *et al.*, (2021) is to calculate the surface of lateral displacement of the swimmer, i.e. the area encompassed by the maximal excursions of the body's amplitude envelope, and thus considers the gradual recruitment of different body parts and accounts for subtleties in swimming behaviour. The surface of lateral displacement was strongly correlated with swimming speed for catfish (*Plotosus lineatus*), emphasising its potential as a valuable parameter for characterising and comparing the swimming amplitudes of anguilliform swimmers.

(3) Larval swimmers and the effect of size

Considerable changes in morphology and ecology can take place from birth to maturity, especially in species that experience metamorphosis. Studies on larval lamprey (McClellan *et al.*, 2016), larval zebrafish (*Danio rerio*) (Müller & Van Leeuwen, 2004), and salamanders (D'Aout & Aerts, 1999) revealed a similar swimming mechanism in larvae and adults, with comparable relationships between their kinematic parameters and employing a similar muscular activation.

However, subtle differences exist. Larvae use a higher swimming frequency (up to 100 Hz) and possess longer specific body λs, closer to 1, than adults which have a proportionately larger lateral surface area of the caudal body. Throughout the various developmental stages, both f and λ gradually decrease as the body grows and the muscles develop, indicating in zebrafish a shift in swimming strategy from cyclic to burst-and-coast swimming (Müller & Van Leeuwen, 2004), as inertial forces become more dominant.

Despite these differences, fish larvae are capable of reaching high absolute speeds, likely because speed plays a vital role in these vulnerable organisms (D'Aout & Aerts, 1999). It has been observed that larvae switch from a viscous hydrodynamic regime to an inertial regime to feed and escape predation. As they grow, they transition to the inertial regime, meaning that larvae and adults move in the same hydrodynamic zone for locomotor behaviours important for survival (Webb & Weihs, 1986). This emphasises the importance of investigating ontogenetic changes in swimming patterns to study the adaptive strategies of aquatic organisms during their early life stages (Herrel & Gibb, 2006). The size of a swimmer is directly related to its swimming kinematics, with the swimming frequency decreasing as L increases (Bainbridge, 1958; Jordan, 1998, Sánchez-Rodríguez, Raufaste & Argentina, 2023).

A numerical study conducted by Tokíc & Yue (2019) used coupled hydrodynamics and muscle contraction characteristics to investigate size-related patterns in oscillatory swimming. In general, larger organisms tend to exhibit a lower

cost of transport (COT), meaning they can travel greater distances with less energy expenditure. However, despite their improved COT, larger swimmers are relatively less efficient in terms of muscle efficiency, indicating that they may require a higher amount of muscular effort to achieve the same swimming performance. Understanding the relationships between size, swimming kinematics, and energy efficiency will be crucial for comprehending the ecological and evolutionary adaptations of aquatic organisms across various body sizes.

(4) Unsteady conditions

(a) *Acceleration and perturbed flow*

The majority of studies measured kinematic parameters during steady swimming, but some recent work has focused on unsteady conditions. Du Clos *et al.* (2019) studied kinematic changes during acceleration from rest in swimming lampreys (*Petromyzon marinus*). Compared to steady swimming, acceleration involves clearly different kinematic patterns, with nearly two times higher mean amplitudes and wavelengths and slower mean wave speeds (Fig. 10). Similar patterns were also reported for accelerating American eels (*Anguilla rostrata*) (Tytell, 2004*a*). Akanyeti *et al.* (2017) further highlighted that the diversity observed for steady swimming among various fish species collapses during acceleration due to a requirement to maximise propulsive efficiency.

A review on unsteady swimming emphasised a growing interest in the effects of artificial altered flows (Liao, 2007). Fishes can adapt their body kinematics in response to perturbations to save energy, leading to a reduction in muscle activity (Liao *et al.*, 2003*a*,*b*).

Additionally, recent investigations focusing on swimming Pacific lamprey (*Entosphenus tridentatus*) shed light on their behaviour when facing obstacles and turbulence (Kirk *et al.*, 2016, 2017). Notably, when exposed to low-level perturbations, lampreys tended to move towards the perturbation, suggesting a potential energy-saving strategy. However, these studies mainly focused on behavioural aspects, and the underlying effects on swimming kinematics are not yet fully understood.

In non-axial flow, i.e. a flow not collinear to the swimming direction, swimming eels showed distinct changes in body kinematics compared to conventional swimming in axial flow (Matar *et al.*, 2012). Specifically, when swimming against non-axial flow, eels displayed asymmetrical body amplitudes relative to their direction of travel. This led to smaller amplitudes on the side where the incoming flow approached the body and larger amplitudes on the opposite side, without any noticeable changes in body wavelength. Again, these investigations primarily focused on behavioural aspects and further research is needed to understand fully the underlying effects on swimming kinematics.

(b) *Backward swimming and viscous environments*

The kinematics of backward swimming have been studied in eels (D'Août & Aerts, 1999; Herrel *et al.*, 2011*a*) and lampreys (Islam *et al.*, 2006). Significant differences in kinematic parameters between forward and backward anguilliform swimming were observed. Specifically, during backward swimming, λ is typically smaller, and the relationship between f and U remains linear but with a substantially higher slope.

The clearest distinction is in the undulation amplitude, which is relatively uniform along the entire length of the body during backward swimming, with even the head exhibiting a high amplitude (Fig. 11). Backward-swimming behaviour differed between two eel species, *Pisodonophis boro* and *Heteroconger hassi*, suggesting that there are interspecific differences, possibly due to morphological and ecological characteristics (Herrel *et al.*, 2011*a*).

During terrestrial locomotion, various aquatic species, including eels (Gillis, 1998*a*), ropefish (Pace & Gibb, 2011), and lungfish (Horner & Jayne, 2014), also exhibit large wave amplitudes along their body. Studies examining swimming behaviour in both viscous water (Horner & Jayne, 2008; Tytell *et al.*, 2023) and sandy shallow water (Pace & Gibb, 2011) have advanced our understanding of how animals move in muddy environments. Notably, the lateral displacement surface gradually increases with higher viscosity and shallower water depth. Swimming cycle frequency can either increase (Pace & Gibb, 2011; Lutek & Standen, 2021) or slightly decrease (Tytell *et al.*, 2023) with viscosity depending on the species. The cycle frequency of the anterior part of the body significantly increases with decreasing

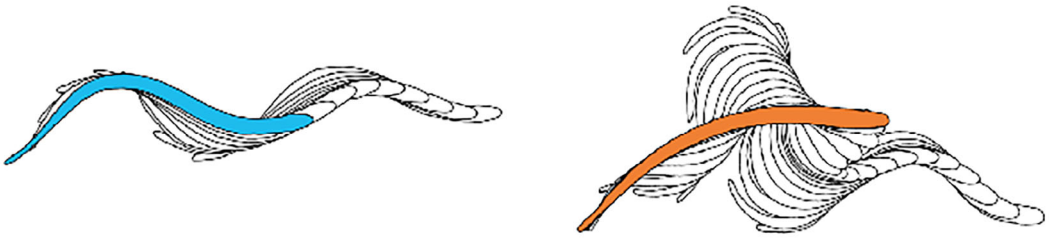

Fig. 10. Differences in body movement parameters between steady swimming (blue) and acceleration (orange) in the lamprey. The black outlines show body outlines during a half tail-beat cycle. Acceleration is characterised by a larger body amplitude and longer body wavelength. Adapted from Du Clos *et al.* (2019).

immersion (Pace & Gibb, 2011). Interestingly, leeches exhibit a different behaviour, with decreased U and f but without changes in swimming amplitude, suggesting that this parameter is more constrained by viscosity compared to lungfish and ropefish (Jordan, 1998).

Interestingly, most kinematics studies of anguilliform swimming report only oscillations in the horizontal plane. However, some anguilliforms, such as lampreys (Lehn, 2019) and snakes (Stin *et al.*, 2023), have been shown to exhibit non-negligible oscillations also in the vertical plane. Moreover, the body of the swimmer can also twist during locomotion (Donatelli, Summers & Tytell, 2017; Gemmell *et al.*, 2016). As highlighted by Lauder (2011), studies investigating 3D kinematics are surprisingly scarce. Complete measurement of kinematics in three dimensions can reveal previously overlooked nuances and complexities, shedding light on the interplay between body morphology, hydrodynamics, and environmental factors, but there is no comprehensive characterisation of the 3D kinematics of anguilliform swimmers available to date.

Certain swimmers, such as snakes, often swim at the water surface (Graham *et al.*, 1987*a*; Hertel, 1966). However, any differences in kinematics between swimming within the water column and at the surface remain unknown. Investigating and understanding these conditions could provide valuable insights into the adaptations of anguilliform swimmers to their specific habitats and locomotion strategies.

IV. HYDRODYNAMICS

The movement of a swimmer, which is controlled by the activation of muscles, has a direct impact on the motion of the surrounding water. Throughout their evolutionary history, aquatic animals have evolved different mechanisms to propel themselves efficiently through water. Natural selection has shaped these propulsive systems, resulting in a wide variety of anatomical and physiological adaptations.

Videler (1993, p. 6) applied Newton's third law to swimming fish, stating that 'Every action of the fish on the water will be opposed by an equal reaction in the opposite direction'. These interactions describe the origin of the thrust of the swimmer, and are essential for a comprehensive understanding of aquatic locomotion. The water that has been put into motion by the submerged body is called the wake. By the action–reaction principle mentioned above, the wake can be seen as the 'footprint' of the swimmer.

(1) Main hydrodynamic interactions

A body submerged underwater experiences two main forces: weight and buoyancy. The balance between them determines whether a body sinks or rises to the surface. To control their buoyancy, fishes employ various strategies, such as gas-filled swim bladders (Videler, 1993; Fath *et al.*, 2023). Most aquatic and semi-aquatic snakes can control their pulmonary volume to regulate their buoyancy (Graham *et al.*, 1987*a*). Other anguilliform swimmers, such as some sharks, do not have a swim bladder, but rely on their fins to manoeuvre (Wilga & Lauder, 2004). With the help of these mechanisms, swimmers can effectively adjust their vertical position within the water column.

When the submerged body starts moving, the flow induced by the swimmer is governed by the Navier–Stokes and incompressibility equations. Their general form can be written as follows, in terms of dimensionless velocity $\boldsymbol{u}$ and pressure p fields:

$$\frac{\partial \boldsymbol{u}}{\partial t} + (\boldsymbol{u}\cdot\boldsymbol{\nabla})\boldsymbol{u} = -\boldsymbol{\nabla}p + \frac{1}{Re}\boldsymbol{\nabla}^2\boldsymbol{u}, \tag{2}$$

$$\boldsymbol{\nabla}\cdot\boldsymbol{u} = 0, \tag{3}$$

where $\mathrm{Re} = LU/\nu$ is the Reynolds number, where v is dynamic viscosity. The dynamic balance between the different terms in Equations (2) and (3) is determined by Re, which measures the relative significance of inertial and viscous forces. For the swimming of macroscopic animals that concerns us here $\mathrm{Re} \gg 1$ and inertial mechanisms dominate. These determine the large-scale flow separations that accompany the periodic body undulations, giving rise to periodic vortex shedding (Lighthill, 1970; Videler, Müller & Stamhuis, 1999). The effects of viscosity, although confined to a thin boundary layer around the animal, are also crucial to the process of vorticity production and are the source of skin friction drag.

Part of the complexity of describing the dynamics of animal swimming comes from the basic observation that water resists motion while at the same time allowing the swimmer to be propelled [see Godoy-Diana & Thiria (2018) for a review]. As the animal moves through the water, it encounters resistance from two main sources: pressure drag and skin-friction drag (Webb, 1975). In anguilliform swimming, where the entire body undulates, both pressure and skin-friction drag are active all along the body of the swimmer (Fig. 12).

A significant part of pressure drag arises from the separated flow behind the moving body as it displaces the fluid in front of it. The displaced fluid is redirected behind the

Fig. 11. Wave amplitudes along the body during forward (A) and backward (B) swimming in the eel *Pisodonophis boro*. Backward swimming involves recruitment of more of the body to contribute to the oscillations. Adapted from Herrel *et al.* (2011*a*).

body, creating a pressure difference known as pressure or form drag (Fig. 12B). As its name suggests, form drag is dependent on the body morphology. A streamlined shape will generate less pressure drag (Hoerner, 1965). In 3D, an additional force known as vortex-induced drag (Raspa *et al.*, 2014) is generated by the trailing vortices that appear due to the pressure at the extremities of the body. Swimmers have a variety of fins to enhance contact with water and therefore optimise thrust *via* this mechanism.

Viscosity causes water particles near the swimmer to move along with it. The velocity of the particles gradually slows down further away from the body surface. This layer of water affected by viscosity is known as the boundary layer. The variation of velocity within the boundary layer creates friction, and the resulting drag is known as skin-friction or viscous drag (Fig. 12C). One way to reduce this viscous drag is to change the body surface properties (see Section II.3).

(2) Hydrodynamic models for undulatory swimming

An initial approach to estimating the forces acting between a swimmer and the surrounding water is to simplify the system by neglecting either inertia (Stokes flow) or viscosity (Euler flow). Given Equations (2) and (3) describing the motion of the fluid, the first case leads to a *resistive* theory where forces depend only on the velocity of the body, while the second is a *reactive* theory, where forces depend on its acceleration. For an undulating body, these model forces act locally on each portion of the body. The global resultant force that gives rise to locomotion then can be computed by summing or integrating all along the body (Godoy-Diana & Thiria, 2018; Wu, 2011).

In the context of inertial undulatory swimmers, the pioneering resistive theory proposed by Taylor (1952) considered the inertial (quadratic) drag along the body. In this model, the swimmer propels itself by 'pushing' against the surrounding fluid. The resistive model is quasi-static, determining forces at any instant based on the instantaneous velocity of each body section. Local drag laws used in this model are derived semi-empirically from cylinders placed in constant-speed flows and do not account for acceleration effects. This approach has been used in many models coupled with muscle mechanics (Cui & Zhang, 2023; McMillen & Holmes, 2006; McMillen *et al.*, 2008; Williams & McMillen, 2015).

The reactive model was proposed by Lighthill (1960, 1971) and Wu (1961), and is widely referred to as the elongated (or slender) body theory. In this model, forces arise from the fluid's reaction to the acceleration imposed by the body undulations. By setting the fluid in motion, the swimmer imparts a net rearward momentum to it, which propels the body forward. The reactive model was developed for swimmers at high *Re* and has been useful in describing carangiform swimming (without a pronounced peduncle), where reactive forces dominate. However, it does not capture fully the streamlined shape and kinematics along the body of anguilliform swimmers which likely use a combination

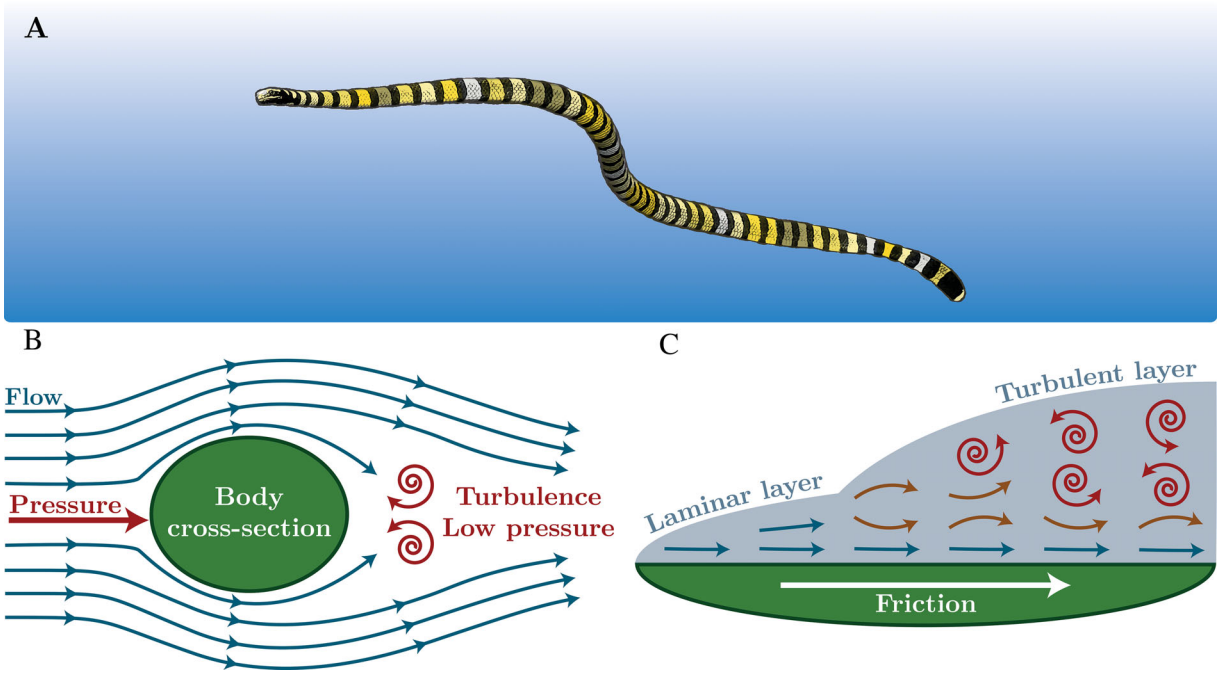

Fig. 12. Fluid–structure interactions during anguilliform swimming. (A) Swimming banded sea krait (*Laticauda colubrina*). (B) The body of the swimming snake can be simplified in two dimensions as a succession of cross-sectional planes along the length of the body. A single cross section is shown, where the separated flow is the source of pressure (form) drag. (C) The boundary layer over any part of the animal in motion, which gives rise to skin-friction drag.

of reactive and resistive forces (Lighthill, 1971). To achieve a better description of propulsion in anguilliform swimmers, it is thus necessary to calculate both inertial and resistive forces (Chen *et al.*, 2011; Piñeirua *et al.*, 2015).

One such approach involves directly computing numerical solutions of the Navier–Stokes equations. This method provides an estimation of both inertial and viscous forces acting on the body of the swimmer and also facilitates the reconstruction of the induced wake. Computational simulations have been conducted for anguilliform swimmers, notably by Kern & Koumoutsakos (2006) on an open-loop problem, i.e. based on predefined inputs and parameters, and Borazjani & Sotiropoulos (2009) and Tytell *et al.* (2010*b*) on a closed-loop problem, i.e. including feedback mechanisms.

(3) Wake characterisation methods

As the wake of a swimmer represents its footprint, a complementary method for studying swimming hydrodynamics is to measure directly the wake under laboratory conditions. There have been considerable advances in flow visualisation techniques and measurements in recent years, especially for applications in experimental biology. Rosen (1959) was the first to use milk as a tracer to visualise the flow around a pearl danio (*Brachydanio albolineatus*) fish. Water snakes (*Natrix natrix*) were also among the earliest animals with published descriptions of their wake (Hertel, 1966). The water was seeded with small particles, enabling visualisation of the production of vortices in the wake. The same technique was used by Gray (1968) to study swimming eels (*Anguilla anguilla*).

Particle image velocimetry (PIV), developed during the past few decades, rapidly found applications in experimental biology. For example, a comprehensive examination of the flow field behind a swimming mullet (*Chelon labrosus*) was performed using methods outlined by Stamhuis & Videler (1995). Shed vortices were identified and energy output estimated (Müller *et al.*, 1997). For anguilliform swimmers, Müller *et al.* (2001) described flow fields for eels (*Anguilla anguilla*). Subsequently, advanced volumetric measurement methods and particle-tracking techniques were developed, including defocusing digital PIV (DDPTV; Pereira *et al.*, 2000), tomographic PIV (TomoPIV; Elsinga *et al.*, 2006), synthetic aperture PIV (SAPIV; Belden *et al.*, 2010), and Lagrangian particle tracking (Shake-the-Box or LPT; Schanz, Gesemann & Schröbler, 2016). These methods enable the 3D reconstruction of a volume, which is particularly advantageous during the study of live animals. It is often unlikely that a swimmer will align perfectly with the measurement plane in 2D PIV, making volumetric methods more suitable.

Volumetric PIV has facilitated the observation of complex wake structures, such as linked vortices in swimming fish (Flammang *et al.*, 2011*a*; Mendelson & Techet, 2015), and the dual ring vortex structure induced by shark tails (Flammang *et al.*, 2011*b*). Furthermore, these techniques have contributed to an understanding of the importance of shed vortices in the manoeuvrability of jellyfish (Gemmell *et al.*, 2015*b*), squid (Bartol *et al.*, 2016), and even jumping fish (Mendelson & Techet, 2018). Some methods provide estimates of hydrodynamic quantities, such as pressure fields, from experimental data (Dabiri *et al.*, 2014). Apart from the unpublished work by Lehn (2019) on swimming lamprey, only Stin *et al.* (2023) have reported experimental volumetric PIV measurements on anguilliform swimmers.

(4) Wake measurements

Experimental measurements of the wake in the horizontal plane by Müller *et al.* (2001) quantified the vortices detached all along the body of a swimming eel. Every time the body wave changes direction, it sheds a vortex from the body to the tip of the tail. Tytell & Lauder (2004) additionally noted that, unlike the downstream flow observed in the wakes of carangiform swimmers, the wake of an eel predominantly exhibited lateral flow.

The resulting 3D structure of the vortices has been revealed to be a hairpin-like structure (Fig. 13) in swimming snakes (Stin *et al.*, 2023) as predicted by computational studies (Borazjani & Sotiropoulos, 2009; Gronskis & Artana, 2016). Kern & Koumoutsakos (2006) also predicted similar results without kinematic input variables by constraining optimization of swimming efficiency. The predicted vortex shedding was, however, more circular. Additionally, Khalid *et al.* (2021) showed that the vortex morphology depends on the body wavelength, λ. A λ in the experimentally observed range for anguilliform swimmers enables the production of vortices more anteriorly along the body, while a higher value of λ centralises vortices more towards the tail.

The ratio of the mean lateral tail velocity to the axial swimming velocity, a non-dimensional number known as the Strouhal number ($St = 2Af/U$), is frequently associated with swimming efficiency (Triantafyllou, Triantafyllou & Rosenbaugh, 1993; Triantafyllou *et al.*, 2000; Taylor, Nudds & Thomas, 2003), with propulsive efficiency being high over a narrow range of St, typically within the interval $0.2 < St < 0.4$. The work of Borazjani & Sotiropoulos (2009) suggested that the wake patterns were influenced by St. Depending on Re, there is a critical St where a transition occurs between two distinct wake patterns. At low St, a single vortex was shed in the wake every half tail-beat cycle, while at higher St, two vortices were shed due to the addition of an extra vortex originating from the body curvature. Notably, anguilliform swimmers typically fall into the latter category (Hertel, 1966; Müller *et al.*, 2001; Tytell & Lauder, 2004).

(5) Swimming mechanism

One proposed mechanism of how the swimmer takes advantage of the vortices produced to propel itself is the 'undulatory pump' model (Blickhan *et al.*, 1992; Videler *et al.*, 1999). This process uses the concept that the swimmer's kinematics are influenced by the surrounding wake. Recent planar PIV investigations on sea lampreys (*Petromyzon marinus*) have mapped the

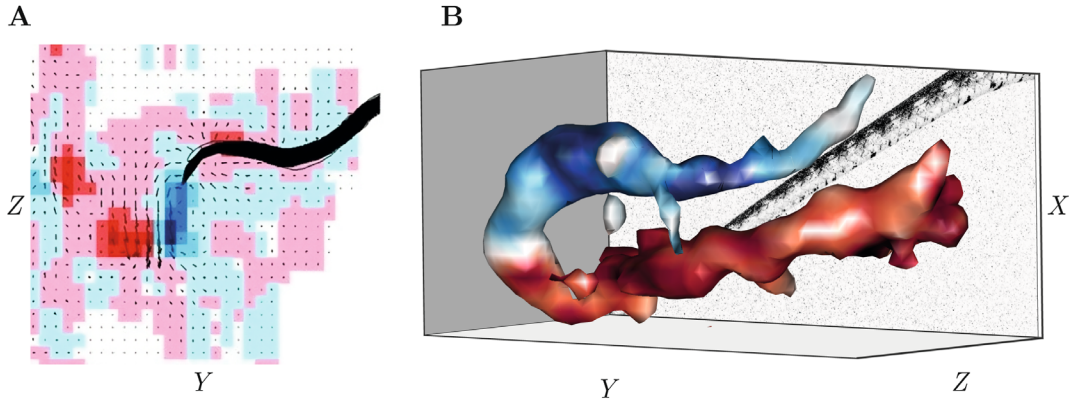

Fig. 13. Wake visualisation of anguilliforms. (A) Flow field of a swimming eel (*Anguilla anguilla*) from Müller *et al.* (2001). (B) Hairpin vortex shed at the tail of a swimming dice snake (*Natrix tessellata*) using volumetric particle image velocimetry (PIV), produced using data in Stin *et al.* (2023).

pressure field surrounding the swimmer (Du Clos *et al.*, 2019; Gemmell *et al.*, 2015*a*, 2016). Through active body bending, the swimmer can control the vorticity and manipulate the surrounding fluid. This bending behaviour generates alternating high- and low-pressure zones along the body, resulting in the localised production of push and pull forces. This process is equivalent to the concept of vortex-induced thrust (Dabiri, 2005; Raspa *et al.*, 2014). In more recent studies, researchers have explored the 3D pressure field in fish wakes (Tu *et al.*, 2022), establishing a closer link between local pressure variations and vortices. Such investigations have not yet been conducted on anguilliform swimmers.

Thrust can be determined experimentally by integrating the pressure components along the body surface, as shown for lampreys (Du Clos *et al.*, 2019; Gemmell *et al.*, 2016). Interestingly, thrust is generated throughout the body, with the second half being the most influential. It was also shown experimentally that the flow velocities increased linearly from the head to the tail in swimming eels (Müller *et al.*, 2001; Tytell & Lauder 2004). Computational studies additionally indicated significant thrust production around the middle of the body during efficient swimming, i.e. swimming when the amount of mean total input power that is transformed into forward motion is maximal (Kern & Koumoutsakos, 2006). Similar predictions were made from a mixed reactive/resistive model using experimental data on swimming leeches (Chen *et al.*, 2011). These findings contrast with predictions of the reactive theory (Lighthill, 1971) that maximum thrust occurs near the tail.

Gazzola *et al.* (2015) introduced the swimming number Sw ($= 2\pi f LA/\nu$), establishing a relationship between the swimmer's gait and its locomotor output, which had been modelled experimentally by Vandenberghe, Zhang & Childress (2004). In the turbulent regime, the ratio Sw/Re approaches 1. However, it was observed that this trend may vary with different gaits, including anguilliform swimming. Figure 14 shows that anguilliform swimmers align quite well with predictions, although predominantly fall below the predicted trend of Sw/Re = 1.

The debate over whether anguilliform swimming is primarily governed by reactive or resistive forces has been a long-standing question. As viscous effects are confined to a thin boundary layer at high Re, Taylor's resistive model is typically applied to microscopic to very small swimmers and Lighthill's reactive model for the majority of macroscopic swimmers. The computations of Borazjani & Sotiropoulos (2009) revealed that the efficiency of a modelled swimming eel drastically dropped when using inviscid flow (i.e. infinite Re). This highlighted that friction has a major impact on thrust generation, even for an eel which could be considered a large enough swimmer to be purely reactive-force driven.

Mixed models from Chen *et al.* (2011) confirmed that resistive forces are dominant for the swimming leech. Piñeirua *et al.* (2015, 2017) further emphasised that inertial and resistive forces depend on the AR as well as the slip ratio (U/V) of the swimmer, and that anguilliform swimmers from Gray (1933*b*), Tytell (2004*b*) and Hess (1983) are governed by resistive forces.

Likely, there are strong variations in the ratio of resistive and reactive forces among different anguilliform swimmers due to variations in external morphology. For example, fish like the longnose gar may exhibit more reactive forces due to their fins. However, an interspecific comparison of the forces acting along the body of anguilliform swimmers is currently lacking.

V. TOWARDS SWIMMING EFFICIENCY

Defining a suitable metric is desirable to estimate swimming efficiency. This is challenging, however, and its complexity can sometimes result in erroneous assessments. A classic illustration of this is observed in 'Gray's Paradox' (Fish, 2006). The two metrics employed most frequently to estimate hydrodynamic efficiency are the Froude efficiency (η) and the hydrodynamic cost of transport (COT_H) defined as:

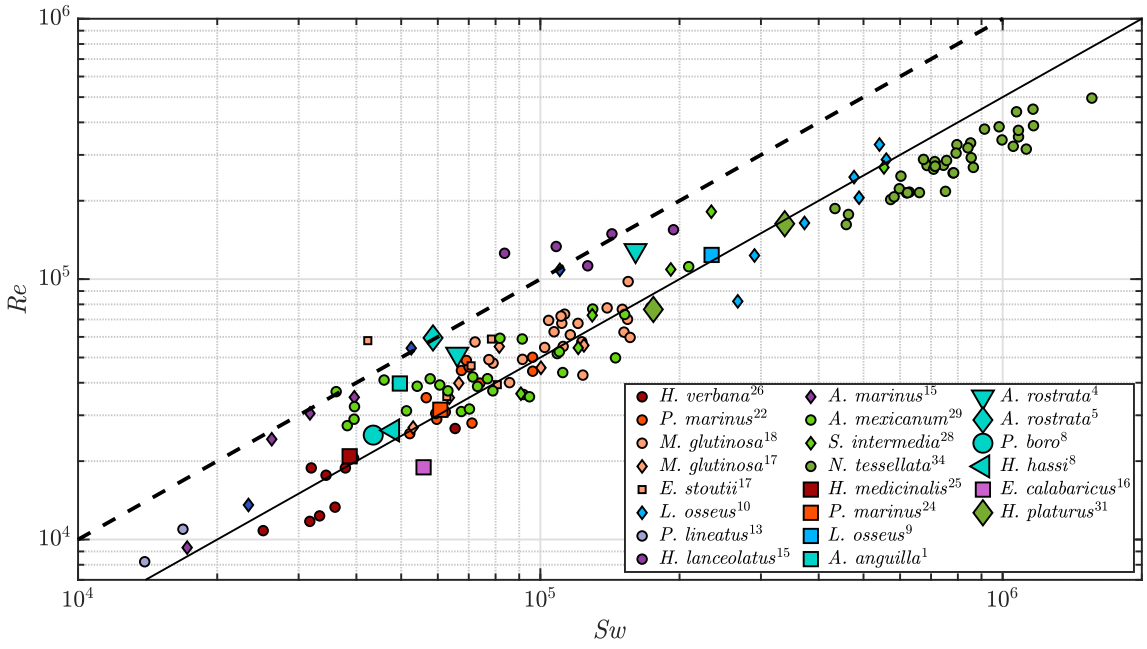

Fig. 14. Compilation of published values for swimming number (*Sw*) against Reynolds number (*Re*) across anguilliform swimmers. Each colour represents an order of swimmers, as compiled in Table 1. Different symbols represent either different species and/or different studies. The solid line is a linear regression fitting the data. The dotted line is the expected trend according to Gazzola *et al.* (2015). Superscript numbers indicate references listed in the footnote to Table 1.

$$\eta = \frac{UT}{P_{\text{in}}}, \tag{4}$$

$$\text{COT}_{\text{H}} = \frac{P_{\text{in}}}{U}, \tag{5}$$

where T is the average thrust and P_{in} is the mechanical power required to swim at speed U. For a review on the use of these metrics, see Maertens, Triantafyllou & Yue (2015).

It should be noted that the metrics mentioned above do not account for metabolic expenditure, which can be estimated by measuring oxygen consumption during swimming (Van Ginneken *et al.*, 2005). Thrust and power are typically estimated using reactive/resistive models or numerical methods, as experimental measurements can pose significant challenges.

The limitation of η in assessing swimming lies in its failure to consider net energy expenditure, which is often conserved in biological systems. By contrast, the hydrodynamic cost of transport is better suited for estimating swimming efficiency, as highlighted in a computational study (Li *et al.*, 2021). However, according to the muscle model proposed by Bhalla *et al.* (2013), the net power generated by the muscles is transferred to the elastic power of the body, which is then dissipated into the fluid during body undulation. Thus, the useful power represents the power spent in undulating the body. To create a fitness measure, Maertens *et al.* (2015) suggested normalising COT_{H} by a towed resistance. These metrics have demonstrated that anguilliform swimming is generally more efficient than carangiform swimming (Borazjani & Sotiropoulos, 2010; Maertens *et al.*, 2015; Tytell *et al.*, 2010*a*). However, to date, a comparison of swimming efficiency among multiple anguilliform swimmers is lacking and filling this gap would provide valuable information.

As previously mentioned, St is commonly associated with propulsive efficiency (Taylor *et al.*, 2003). It has been demonstrated that η reaches a maximum within a narrow range of St for oscillating foils (Triantafyllou *et al.*, 1993), which holds true for non-anguilliform swimmers. However, several comparative studies have highlighted that anguilliform swimmers often lie outside the range of optimal St (Eloy, 2012; Nangia *et al.*, 2017; Van Weerden *et al.*, 2014). This finding contradicts the notion that anguilliform swimmers are generally more efficient than carangiform swimmers. The discrepancy arises because St includes only the tail-beat amplitude in its definition. While carangiform swimmers predominantly use their caudal fins, which can be approximated by the foils of Triantafyllou *et al.*, (1993), St fails to account for the gradually increasing amplitude along the body of anguilliform swimmers. Therefore, St is not well suited for estimating the efficiency of anguilliform swimmers.

Measuring swimming efficiency in live animals is challenging. As highlighted by Lauder (2022), robots are slowly becoming valuable tools for conducting comparative studies, as they allow for easy tuning of swimming parameters and a deeper understanding of the performance effects of specific organismal traits.

VI. CONCLUSIONS

(1) Our study highlights that anguilliform swimmers display diversity in both their internal structure and external shape.

In vivo experiments and models have demonstrated how anguilliform swimmers are propelled by their musculotendinous system, generating motion. The shape, stiffness, and flexibility of the swimmers influence the surrounding fluid. The impact of the wetted surface topology on swimming performance remains poorly known.

(2) A comparison of data from a large number of studies on the kinematics of anguilliform swimmers shows that, despite intra- and interspecific variation, the tail-beat frequency and body wave speed, as functions of swimming speed, follow a similar linear trend for all studied anguilliform swimmers. While they typically swim with a wavelength less than 1, swimming speed can vary greatly among species. Notably, there are few studies on the 3D kinematics of anguilliform swimming.

(3) A survey of flow visualisation studies on the wake of anguilliform swimmers reveals that the resulting hydrodynamic signature comprises vortex loops. Mechanistic hypotheses suggest that through active body bending, some anguilliform swimmers can control vorticity and manipulate the surrounding fluid. Nevertheless, the correlation between the wake of the swimmer and its swimming performance is not fully understood and 3D measurements across various anguilliform species are lacking.

(4) There is no real consensus on the best metric to quantify hydrodynamic efficiency. Estimating swimming efficiency and comparing it among different anguilliform swimmers, while also establishing correlations with anatomical features, kinematic output, and hydrodynamic signature, could provide valuable insights into their evolutionary adaptations. Such findings could potentially drive advances in diverse fields, ranging from biology to robotics.

VII. REFERENCES

Akanyeti, O., Di Santo, V., Goerig, E., Wainwright, D. K., Liao, J. C., Castro-Santos, T. & Lauder, G. V. (2022). Fish-inspired segment models for undulatory steady swimming. *Bioinspiration & Biomimetics* **17**, 046007.

Akanyeti, O., Putney, J., Yanagitsuru, Y. R., Lauder, G. V., Stewart, W. J. & Liao, J. C. (2017). Accelerating fishes increase propulsive efficiency by modulating vortex ring geometry. *Proceedings of the National Academy of Sciences* **114**, 13828–13833.

Akat, E., Yenmiş, M., Pombal, M. A., Molist, P., Megias, M., Arman, S., Veselý, M., Anderson, R. & Ayaz, D. (2022). Comparison of vertebrate skin structure at class level: a review. *The Anatomical Record* **305**, 3543–3608.

Altringham, J. D. & Ellerby, D. J. (1999). Fish swimming: patterns in muscle function. *Journal of Experimental Biology* **202**, 3397–3403.

Anastasiadis, A., Paez, L., Melo, K., Tytell, E. D., Ijspeert, A. J. & Mulleners, K. (2023). Identification of the trade-off between speed and efficiency in undulatory swimming using a bio-inspired robot. *Scientific Reports* **13**, 15032.

Anderson, E. J., Mcgillis, W. R. & Grosenbaugh, M. A. (2001). The boundary layer of swimming fish. *Journal of Experimental Biology* **204**, 81–102.

Aubret, F. & Shine, R. (2008). The origin of evolutionary innovations: locomotor consequences of tail shape in aquatic snakes. *Functional Ecology* **22**, 317–322.

Bainbridge, R. (1958). The speed of swimming of fish as related to size and to the frequency and amplitude of the tail beat. *Journal of Experimental Biology* **35**, 109–133.

Bale, R., Neveln, I. D., Bhalla, A. P. S., MacIver, M. A. & Patankar, N. A. (2015). Convergent evolution of mechanically optimal locomotion in aquatic invertebrates and vertebrates. *PLoS Biology* **13**, e1002123.

Bartol, I. K., Krueger, P. S., Jastrebsky, R. A., Williams, S. & Thompson, J. T. (2016). Volumetric flow imaging reveals the importance of vortex ring formation in squid swimming tail-first and arms-first. *Journal of Experimental Biology* **219**, 392–403.

Belden, J., Truscott, T. T., Axiak, M. C. & Techet, A. H. (2010). Three-dimensional synthetic aperture particle image velocimetry. *Measurement Science and Technology* **21**, 125403.

Bhalla, A. P. S., Griffith, B. E. & Patankar, N. A. (2013). A forced damped oscillation framework for undulatory swimming provides new insights into how propulsion arises in active and passive swimming. *PLoS Computational Biology* **9**, e1003097.

Blickhan, R., Krick, C., Zehren, D., Nachtigall, W. & Breithaupt, T. (1992). Generation of a vortex chain in the wake of a subundulatory swimmer. *Naturwissenschaften* **79**, 220–221.

Blight, A. R. (1977). The muscular control of vertebrate swimming movements. *Biological Reviews* **52**, 181–218.

Boomsma, A. & Sotiropoulos, F. (2016). Direct numerical simulation of sharkskin denticles in turbulent channel flow. *Physics of Fluids* **28**, 035106.

Borazjani, I. & Sotiropoulos, F. (2009). Numerical investigation of the hydrodynamics of anguilliform swimming in the transitional and inertial flow regimes. *Journal of Experimental Biology* **212**, 576–592.

Borazjani, I. & Sotiropoulos, F. (2010). On the role of form and kinematics on the hydrodynamics of self-propelled body/caudal fin swimming. *Journal of Experimental Biology* **213**, 89–107.

Bowtell, G. & Williams, T. L. (1991). Anguilliform body dynamics: modelling the interaction between muscle activation and body curvature. *Philosophical Transactions of the Royal Society of London Series B: Biological Sciences* **334**, 385–390.

Bowtell, G. & Williams, T. L. (1994). Anguilliform body dynamics: a continuum model for the interaction between muscle activation and body curvature. *Journal of Mathematical Biology* **32**, 83–91.

Breder, C. M. (1926). The locomotion of fishes. *Zoologica* **4**, 159–297.

Brischoux, F., Kato, A., Ropert-Coudert, Y. & Shine, R. (2010). Swimming speed variation in amphibious seasnakes (*Laticaudinae*): a search for underlying mechanisms. *Journal of Experimental Marine Biology and Ecology* **394**, 116–122.

Chao, L. M., Alam, M. M. & Cheng, L. (2022). Hydrodynamic performance of slender swimmer: effect of travelling wavelength. *Journal of Fluid Mechanics* **947**, A8.

Chen, J., Friesen, W. O. & Iwasaki, T. (2011). Mechanisms underlying rhythmic locomotion: body-fluid interaction in undulatory swimming. *Journal of Experimental Biology* **214**, 561–574.

Chen, J., Friesen, W. O. & Iwasaki, T. (2012). Mechanisms underlying rhythmic locomotion: interactions between activation, tension and body curvature waves. *Journal of Experimental Biology* **215**, 211–219.

Clark, A. J., Crawford, C. H., King, B. D., Demas, A. M. & Uyeno, T. A. (2016). Material properties of hagfish skin, with insights into knotting behaviors. *The Biological Bulletin* **230**, 243–256.

Coughlin, D. J. (2002). Aerobic muscle function during steady swimming in fish. *Fish and Fisheries* **3**, 63–78.

Cui, Z. & Zhang, X. (2023). Computational study of stiffness-tuning strategies in anguilliform fish. *Biomimetics* **8**, 263.

Dabiri, J. O. (2005). On the estimation of swimming and flying forces from wake measurements. *Journal of Experimental Biology* **208**, 3519–3532.

Dabiri, J. O., Bose, S., Gemmell, B. J., Colin, S. P. & Costello, J. H. (2014). An algorithm to estimate unsteady and quasi-steady pressure fields from velocity field measurements. *Journal of Experimental Biology* **217**, 331–336.

Danos, N., Fisch, N. & Gemballa, S. (2008). The musculotendinous system of an anguilliform swimmer: muscles, myosepta, dermis, and their interconnections in *Anguilla rostrata*. *Journal of Morphology* **269**, 29–44.

D'Août, K. (1997). Kinematics and efficiency of steady swimming in adult axolotls (*Ambystoma mexicanum*). *Journal of Experimental Biology* **200**, 1863–1871.

D'Août, K. & Aerts, P. (1999). A kinematic comparison of forward and backward swimming in the eel *Anguilla Anguilla*. *Journal of Experimental Biology* **202**, 1511–1521.

D'Aout, K. & Aerts, P. (1999). The kinematics of voluntary steady swimming of hatchling and adult axolotls (*Ambystoma mexicanum* Shaw, 1789). *Belgian Journal of Zoology* **129**, 305–316.

D'Août, K., Curtin, N., Williams, T. & Aerts, P. (2001). Mechanical properties of red and white swimming muscles as a function of the position along the body of the eel *Anguilla Anguilla*. *Journal of Experimental Biology* **204**, 2221–2230.

Dean, B. & Bhushan, B. (2010). Shark-skin surfaces for fluid-drag reduction in turbulent flow: a review. *Philosophical Transactions of the Royal Society A: Mathematical, Physical and Engineering Sciences* **368**, 4775–4806.

Devaere, S., Jansen, G., Adriaens, D. & Weekers, P. (2007). Phylogeny of the African representatives of the catfish family *Clariidae* (*Teleostei*, *Siluriformes*) based on a combined analysis: independent evolution towards anguilliformity. *Journal of Zoological Systematics and Evolutionary Research* **45**, 214–229.

Di Santo, V., Goerig, E., Wainwright, D. K., Akanyeti, O., Liao, J. C., Castro-Santos, T. & Lauder, G. V. (2021). Convergence of undulatory swimming kinematics across a diversity of fishes. *Proceedings of the National Academy of Sciences* **118**, e2113206118.

Ding, Y., Sharpe, S. S., Masse, A. & Goldman, D. I. (2012). Mechanics of undulatory swimming in a frictional fluid. *PLoS Computational Biology* **8**, e1002810.

Ding, Y., Sharpe, S. S., Wiesenfeld, K. & Goldman, D. I. (2013). Emergence of the advancing neuromechanical phase in a resistive force dominated medium. *Proceedings of the National Academy of Sciences* **110**, 10123–10128.

Domel, A. G., Domel, G., Weaver, J. C., Saadat, M., Bertoldi, K. & Lauder, G. V. (2018). Hydrodynamic properties of biomimetic shark skin: effect of denticle size and swimming speed. *Bioinspiration & Biomimetics* **13**, 056014.

Donatelli, C. M., Summers, A. P. & Tytell, E. D. (2017). Long-axis twisting during locomotion of elongate fishes. *Journal of Experimental Biology* **220**, 3632–3640.

Du Clos, K. T., Dabiri, J. O., Costello, J. H., Colin, S. P., Morgan, J. R., Fogerson, S. M. & Gemmell, B. J. (2019). Thrust generation during steady swimming and acceleration from rest in anguilliform swimmers. *Journal of Experimental Biology* **222**, jeb212464.

Ehrenstein, U. & Eloy, C. (2013). Skin friction on a moving wall and its implications for swimming animals. *Journal of Fluid Mechanics* **718**, 321–346.

Eloy, C. (2012). Optimal Strouhal number for swimming animals. *Journal of Fluids and Structures* **30**, 205–218.

Eloy, C. (2013). On the best design for undulatory swimming. *Journal of Fluid Mechanics* **717**, 48–89.

Elsinga, G. E., Scarano, F., Wieneke, B. & Van Oudheusden, B. W. (2006). Tomographic particle image velocimetry. *Experiments in Fluids* **41**, 933–947.

Fath, M. A., Nguyen, S., Donahue, J., Mcmenamin, S. & Tytell, E. D. (2023). Static stability and swim bladder volume in the bluegill sunfish *Lepomis macrochirus*. *Integrative Organismal Biology* **5**, obad005.

Feilich, K. L. (2016). Correlated evolution of body and fin morphology in the cichlid fishes. *Evolution* **70**, 2247–2267.

Fish, F. & Lauder, G. V. (2006). Passive and active flow control by swimming fishes and mammals. *Annual Review of Fluid Mechanics* **38**, 193–224.

Fish, F. E. (2006). The myth and reality of Gray's paradox: implication of dolphin drag reduction for technology. *Bioinspiration & Biomimetics* **1**, R17.

Flammang, B. E., Lauder, G. V., Troolin, D. R. & Strand, T. (2011*b*). Volumetric imaging of shark tail hydrodynamics reveals a three-dimensional dual-ring vortex wake structure. *Proceedings of the Royal Society B: Biological Sciences* **278**, 3670–3678.

Flammang, B. E., Lauder, G. V., Troolin, D. R. & Strand, T. E. (2011*a*). Volumetric imaging of fish locomotion. *Biology Letters* **7**, 695–698.

Frolich, L. M. & Biewener, A. A. (1992). Kinematic and electromyographic analysis of the functional role of the body axis during terrestrial and aquatic locomotion in the salamander *Ambystoma tigrinum*. *Journal of Experimental Biology* **162**, 107–130.

Gans, C. (1975). Tetrapod limblessness: evolution and functional corollaries. *American Zoologist* **15**, 455–467.

Gazzola, M., Argentina, M. & Mahadevan, L. (2015). Gait and speed selection in slender inertial swimmers. *Proceedings of the National Academy of Sciences* **112**, 3874–3879.

Gemballa, S. & Vogel, F. (2002). Spatial arrangement of white muscle fibers and myoseptal tendons in fishes. *Comparative Biochemistry and Physiology Part A: Molecular & Integrative Physiology* **133**, 1013–1037.

Gemmell, B. J., Colin, S. P., Costello, J. H. & Dabiri, J. O. (2015*a*). Suction-based propulsion as a basis for efficient animal swimming. *Nature Communications* **6**, 8790.

Gemmell, B. J., Fogerson, S. M., Costello, J. H., Morgan, J. R., Dabiri, J. O. & Colin, S. P. (2016). How the bending kinematics of swimming lampreys build negative pressure fields for suction thrust. *Journal of Experimental Biology* **219**, 3884–3895.

Gemmell, B. J., Troolin, D. R., Costello, J. H., Colin, S. P. & Satterlie, R. A. (2015*b*). Control of vortex rings for manoeuvrability. *Journal of the Royal Society Interface* **12**, 20150389.

Gillis, G. B. (1996). Undulatory locomotion in elongate aquatic vertebrates: anguilliform swimming since sir James Gray. *American Zoologist* **36**, 656–665.

Gillis, G. B. (1997). Anguilliform locomotion in an elongate salamander (*Siren intermedia*): effects of speed on axial undulatory movements. *Journal of Experimental Biology* **200**, 767–784.

Gillis, G. B. (1998*a*). Environmental effects on undulatory locomotion in the American eel *Anguilla rostrata*: kinematics in water and on land. *Journal of Experimental Biology* **201**, 949–961.

Gillis, G. B. (1998*b*). Neuromuscular control of anguilliform locomotion: patterns of red and white muscle activity during swimming in the American eel *Anguilla rostrata*. *Journal of Experimental Biology* **201**, 3245–3256.

Godoy-Diana, R. & Thiria, B. (2018). On the diverse roles of fluid dynamic drag in animal swimming and flying. *Journal of the Royal Society Interface* **15**, 20170715.

Graham, J., Gee, J., Motta, J. & Rubinoff, I. (1987*a*). Subsurface buoyancy regulation by the sea snake *Pelamis platurus*. *Physiological Zoology* **60**, 251–261.

Graham, J. B., Lowell, W. R., Rubinoff, I. & Motta, J. (1987*b*). Surface and subsurface swimming of the sea snake *Pelamis platurus*. *Journal of Experimental Biology* **127**, 27–44.

Gravish, N. & Lauder, G. V. (2018). Robotics-inspired biology. *Journal of Experimental Biology* **221**, jeb138438.

Gray, J. (1933*a*). Studies in animal locomotion: I. The movement of fish with special reference to the eel. *Journal of Experimental Biology* **10**, 88–104.

Gray, J. (1933*b*). Studies in animal locomotion. II. The relationship between waves of muscular con- traction and the propulsive mechanism of the eel. *Journal of Experimental Biology* **10**, 386–390.

Gray, J. (1968). *Animal locomotion*. Weidenfeld & Nicolson, London.

Grillner, S. & Kashin, S. (1976). On the generation and performance of swimming in Fish. In *Neural Control of Locomotion. Advances in Behavioral Biology* (Volume **18**, eds R. M. Herman, S. Grillner, P. S. G. Stein and D. G. Stuart), pp. 181–201. Springer, New York.

Gronskis, A. & Artana, G. (2016). A simple and efficient direct forcing immersed boundary method combined with a high order compact scheme for simulating flows with moving rigid boundaries. *Computers & Fluids* **124**, 86–104.

Hamlet, C. L., Hoffman, K. A., Tytell, E. D. & Fauci, L. J. (2018). The role of curvature feedback in the energetics and dynamics of lamprey swimming: a closed-loop model. *PLoS Computational Biology* **14**, e1006324.

Hebrank, M. R. (1980). Mechanical properties and locomotor functions of eel skin. *Biological Bulletin* **158**, 58–68.

Herrel, A., Choi, H. F., De Schepper, N., Aerts, P. & Adriaens, D. (2011*a*). Kinematics of swimming in two burrowing anguilliform fishes. *Zoology* **114**, 78–84.

Herrel, A., Choi, H. F., Dumont, E., De Schepper, N., Vanhooydonck, B., Aerts, P. & Adriaens, D. (2011*b*). Burrowing and subsurface locomotion in anguilliform fish: behavioral specializations and mechanical constraints. *Journal of Experimental Biology* **214**, 1379–1385.

Herrel, A. & Gibb, A. C. (2006). Ontogeny of performance in vertebrates. *Physiological and Biochemical Zoology* **79**, 1–6.

Hertel, H. (1966). *Structure, Form, Movement*, pp. 178–184. Reinhold Publishing, New York.

Hess, F. (1983). Bending moments and muscle power in swimming fish. In *Proceedings of the 8th Australasian Fluid Mechanics Conference* (Volume **2**), pp. 12A1–12A3. University of Newcastle, New South Wales.

Hoar, W. S. & Randall, D. J. (1978). *Fish Physiology: Locomotion*. Academic Press, London.

Hoerner, S. F. (1965). *Fluid Dynamic Drag: Practical Information on Aerodynamic Drag and Hydrodynamic Resistance*. Hoerner Fluid Dynamics, Brick Town, New Jersey.

Hoover, A. P., Daniels, J., Nawroth, J. C. & Katija, K. (2021). A computational model for tail undulation and fluid transport in the giant larvacean. *Fluids* **6**, 88.

Horner, A. M. & Jayne, B. C. (2008). The effects of viscosity on the axial motor pattern and kinematics of the African lungfish (*Protopterus annectens*) during lateral undulatory swimming. *Journal of Experimental Biology* **211**, 1612–1622.

Horner, A. M. & Jayne, B. C. (2014). Lungfish axial muscle function and the vertebrate water to land transition. *PLoS One* **9**, e96516.

Islam, S. S., Zelenin, P. V., Orlovsky, G. N., Grillner, S. & Deliagina, T. G. (2006). Pattern of motor coordination underlying backward swimming in the lamprey. *Journal of Neurophysiology* **96**, 451–460.

Jacobs, R. P. & O'Donnell, E. B. (2009). *A Pictorial Guide to Freshwater Fishes of Connecticut*, Edition (Volume **42**). Connecticut Department of Environmental Protection, Hartford, CT.

Jayne, B. C. (1985). Swimming in constricting (*Elaphe g. guttata*) and nonconstricting (*Nerodia fasciata pictiventris*) colubrid snakes. *Copeia* **1985**, 195.

Jayne, B. C. (1988*a*). Mechanical behaviour of snake skin. *Journal of Zoology* **214**, 125–140.

Jayne, B. C. (1988*b*). Muscular mechanisms of snake locomotion: an electromyographic study of lateral undulation of the Florida banded water snake (*Nerodia fasciata*) and the yellow rat snake (*Elaphe obsoleta*). *Journal of Morphology* **197**, 159–181.

Jordan, C. E. (1998). Scale effects in the kinematics and dynamics of swimming leeches. *Canadian Journal of Zoology* **76**, 1869–1877.

Kayan, V., Kozlov, L. & Pyatetskii, V. (1978). Kinematic characteristics of the swimming of certain aquatic animals. *Fluid Dynamics* **13**, 641–646.

Kenaley, C. P., Sanin, A., Ackerman, J., Yoo, J. & Alberts, A. (2018). Skin stiffness in ray finned fishes: contrasting material properties between species and body regions. *Journal of Morphology* **279**, 1419–1430.

Kennedy, E. L., Patel, R. P., Perez, C. P., Clubb, B. L., Uyeno, T. A. & Clark, A. J. (2021). Comparative biomechanics of hagfish skins: diversity in material, morphology, and movement. *Zoology* **145**, 125888.

Kern, S. & Koumoutsakos, P. (2006). Simulations of optimized anguilliform swimming. *Journal of Experimental Biology* **209**, 4841–4857.

Khalid, M. S. U., Wang, J., Akhtar, I., Dong, H., Liu, M. & Hemmati, A. (2021). Why do anguilliform swimmers perform undulation with wavelengths shorter than their bodylengths? *Physics of Fluids* **33**, 031911.

Khalid, M. S. U., Wang, J., Dong, H. & Liu, M. (2020). Flow transitions and mapping for undulating swimmers. *Physical Review Fluids* **5**, 063104.
Kirk, M., Caudill, C., Tonina, D. & Syms, J. (2016). Effects of water velocity, turbulence and obstacle length on the swimming capabilities of adult Pacific lamprey. *Fisheries Management and Ecology* **23**, 356–366.
Kirk, M. A., Caudill, C. C., Syms, J. C. & Tonina, D. (2017). Context-dependent responses to turbulence for an anguilliform swimming fish, Pacific lamprey, during passage of an experimental vertical-slot weir. *Ecological Engineering* **106**, 296–307.
Lauder, G. V. (2011). Swimming hydrodynamics: ten questions and the technical approaches needed to resolve them. *Experiments in Fluids* **51**, 23–35.
Lauder, G. V. (2015). Fish locomotion: recent advances and new directions. *Annual Review of Marine Science* **7**, 521–545.
Lauder, G. V. (2022). Robotics as a comparative method in ecology and evolutionary biology. *Integrative and Comparative Biology* **62**, 721–734.
Lauder, G. V., Wainwright, D. K., Domel, A. G., Weaver, J. C., Wen, L. & Bertoldi, K. (2016). Structure, biomimetics, and fluid dynamics of fish skin surfaces. *Physical Review Fluids* **1**, 060502.
Lehn, A. M. (2019). Volumetric analysis of lamprey hydrodynamics using synthetic aperture particle image velocimetry. PhD thesis: Massachusetts Institute of Technology.
Li, G., Liu, G., Leng, D., Fang, X., Li, G. & Wang, W. (2023). Underwater undulating propulsion biomimetic robots: a review. *Biomimetics* **8**, 318.
Li, G., Liu, H., Müller, U. K., Voesenek, C. J. & Van Leeuwen, J. L. (2021). Fishes regulate tail- beat kinematics to minimize speed-specific cost of transport. *Proceedings of the Royal Society B* **288**, 20211601.
Liao, J. C. (2002). Swimming in needlefish (Belonidae): anguilliform locomotion with fins. *Journal of Experimental Biology* **205**, 2875–2884.
Liao, J. C. (2007). A review of fish swimming mechanics and behaviour in altered flows. *Philosophical Transactions of the Royal Society of London. Series B, Biological Sciences* **362**, 1973–1993.
Liao, J. C., Beal, D. N., Lauder, G. V. & Triantafyllou, M. S. (2003*a*). Fish exploiting vortices decrease muscle activity. *Science* **302**, 1566–1569.
Liao, J. C., Beal, D. N., Lauder, G. V. & Triantafyllou, M. S. (2003*b*). The Kármán gait: novel body kinematics of rainbow trout swimming in a vortex street. *Journal of Experimental Biology* **206**, 1059–1073.
Lighthill, M. J. (1960). Note on the swimming of slender fish. *Journal of Fluid Mechanics* **9**, 305–317.
Lighthill, M. J. (1969). Hydromechanics of aquatic animal propulsion. *Annual Review of Fluid Mechanics* **1**, 413–446.
Lighthill, M. J. (1970). Aquatic animal propulsion of high hydromechanical efficiency. *Journal of Fluid Mechanics* **44**, 265–301.
Lighthill, M. J. (1971). Large-amplitude elongated-body theory of fish locomotion. *Proceedings of the Royal Society of London. Series B. Biological Sciences* **179**, 125–138.
Lighthill, M. J. (1975). *Mathematical Biofluiddynamics*. SIAM, Philadelphia.
Lim, J. L. & Winegard, T. M. (2015). Diverse anguilliform swimming kinematics in Pacific hagfish (*Eptatretus stoutii*) and Atlantic hagfish (*Myxine glutinosa*). *Canadian Journal of Zoology* **93**, 213–223.
Lindsey, C. C. (1978). Form, function, and locomotory habits in fish. In *Fish Physiology: Locomotion* (Volume **7**, eds W. S. Hoar and D. J. Randall), pp. 1–100. Academic Press, London.
Liu, G., Yuan, Z., Qiu, Z., Feng, S., Xie, Y., Leng, D. & Tian, X. (2020). A brief review of bio-inspired surface technology and application toward underwater drag reduction. *Ocean Engineering* **199**, 106962.
Long, J. H. (1998). Muscles, elastic energy, and the dynamics of body stiffness in swimming eels. *American Zoologist* **38**(4), 771–792.
Long, J. H., Hale, M. E., McHenry, M. J. & Westneat, M. K. (1996). Functions of fish skin: flexural stiffness and steady swimming of longnose gar *Lepisosteus osseus*. *Journal of Experimental Biology* **199**, 2139–2151.
Long, J. H., Koob-Emunds, M., Sinwell, B. & Koob, T. J. (2002). The notochord of hagfish *Myxine glutinosa*: visco-elastic properties and mechanical functions during steady swimming. *Journal of Experimental Biology* **205**, 3819–3831.
Long, J. H., Shepherd, W. & Root, R. (1997). Manueuverability and reversible propulsion: how eel- like fish swim forward and backward using travelling body waves. In *Proceedings of the Special Session on Bio-Engineering Research Related to Autonomous Underwater Vehicles, 10th International Symposium on Unmanned Untethered Submersible Technology*, pp. 118–134. Office of Navel Research, Arlington, VA.
Lutek, K. & Standen, E. M. (2021). Increasing viscosity helps explain locomotor control in swimming *Polypterus senegalus*. *Integrative Organismal Biology* **3**, obab024.
Maertens, A., Triantafyllou, M. S. & Yue, D. K. (2015). Efficiency of fish propulsion. *Bioinspiration & Biomimetics* **10**, 046013.
Matar, Y., Candelier, F. & Solliec, C. (2012). How the kinematic swimming of European eel *Anguilla Anguilla* changes from axial to non-axial velocity flow. *International Journal of Bioengineering and Life Sciences* **6**, 100–104.
Mathou, A., Bonnet, X., Daoues, K., Ksas, R. & Herrel, A. (2023). Evolutionary convergence of muscle architecture in relation to locomotor ecology in snakes. *Journal of Anatomy* **242**, 862–871.
McClellan, A. D., Pale, T., Messina, J. A., Buso, S. & Shebib, A. (2016). Similarities and differences for swimming in larval and adult lampreys. *Physiological and Biochemical Zoology* **89**, 294–312.
McMillen, T. & Holmes, P. (2006). An elastic rod model for anguilliform swimming. *Journal of Mathematical Biology* **53**, 843–886.
McMillen, T., Williams, T. & Holmes, P. (2008). Nonlinear muscles, passive viscoelasticity and body taper conspire to create neuromechanical phase lags in anguilliform swimmers. *PLoS Computational Biology* **4**, e1000157.
Mehta, R. S., Ward, A. B., Alfaro, M. E. & Wainwright, P. C. (2010). Elongation of the body in eels. *Integrative and Comparative Biology* **50**, 1091–1105.
Mendelson, L. & Techet, A. H. (2015). Quantitative wake analysis of a freely swimming fish using 3D synthetic aperture PIV. *Experiments in Fluids* **56**, 1–19.
Mendelson, L. & Techet, A. H. (2018). Multi-camera volumetric PIV for the study of jumping fish. *Experiments in Fluids* **59**, 10.
Ming, T., Jin, B., Song, J., Luo, H., Du, R. & Ding, Y. (2019). 3D computational models explain muscle activation patterns and energetic functions of internal structures in fish swimming. *PLoS Computational Biology* **15**, e1006883.
Miyazaki, M., Hirai, Y., Moriya, H., Shimomura, M., Miyauchi, A. & Liu, H. (2018). Biomimetic riblets inspired by sharkskin denticles: digitizing, modeling and flow simulation. *Journal of Bionic Engineering* **15**, 999–1011.
Müller, U. K., Smit, J., Stamhuis, E. J. & Videler, J. J. (2001). How the body contributes to the wake in undulatory fish swimming: flow fields of a swimming eel (*Anguilla Anguilla*). *Journal of Experimental Biology* **204**, 2751–2762.
Müller, U. K., Van Den Heuvel, B. L. E., Stamhuis, E. J. & Videler, J. J. (1997). Fish foot prints: morphology and energetics of the wake behind a continuously swimming mullet (*Chelon labrosus* Risso). *Journal of Experimental Biology* **200**, 2893–2906.
Müller, U. K. & Van Leeuwen, J. L. (2004). Swimming of larval zebrafish: ontogeny of body waves and implications for locomotory development. *Journal of Experimental Biology* **207**, 853–868.
Munk, Y. (2008). Kinematics of swimming garter snakes (*Thamnophis sirtalis*). *Comparative Biochemistry and Physiology Part A, Molecular & Integrative Physiology* **150**, 131–135.
Nangia, N., Bale, R., Chen, N., Hanna, Y. & Patankar, N. A. (2017). Optimal specific wavelength for maximum thrust production in undulatory propulsion. *PLoS One* **12**, e0179727.
Nelson, J. S., Grande, T. C. & Wilson, M. V. (1976). *Fishes of the World*. John Wiley & Sons, Hoboken, NJ.
Nowroozi, B. N. & Brainerd, E. L. (2014). Importance of mechanics and kinematics in determining the stiffness contribution of the vertebral column during body-caudal-fin swimming in fishes. *Zoology* **117**, 28–35.
Pace, C. M. & Gibb, A. C. (2011). Locomotor behavior across an environmental transition in the ropefish, *Erpetoichthys calabaricus*. *Journal of Experimental Biology* **214**, 530–537.
Pattishall, A. & Cundall, D. (2008). Dynamic changes in body form during swimming in the water snake *Nerodia sipedon*. *Zoology* **111**, 48–61.
Pedley, T. & Hill, S. (1999). Large-amplitude undulatory fish swimming: fluid mechanics coupled to internal mechanics. *Journal of Experimental Biology* **202**, 3431–3438.
Pereira, F., Gharib, M., Dabiri, D. & Modarress, D. (2000). Defocusing digital particle image velocimetry: a 3-component 3-dimensional DPIV measurement technique. Application to bubbly flows. *Experiments in Fluids* **29**, S078–S084.
Piñeirua, M., Godoy-Diana, R. & Thiria, B. (2015). Resistive thrust production can be as crucial as added mass mechanisms for inertial undulatory swimmers. *Physical Review E* **92**, 021001.
Piñeirua, M., Thiria, B. & Godoy-Diana, R. (2017). Modelling of an actuated elastic swimmer. *Journal of Fluid Mechanics* **829**, 731–750.
Ramananarivo, S., Godoy-Diana, R. & Thiria, B. (2013). Passive elastic mechanism to mimic fish-muscle action in anguilliform swimming. *Journal of the Royal Society Interface* **10**, 20130667.
Raspa, V., Ramananarivo, S., Thiria, B. & Godoy-Diana, R. (2014). Vortex-induced drag and the role of aspect ratio in undulatory swimmers. *Physics of Fluids* **26**, 041701.
Root, R. G., Courtland, H. W., Shepherd, W. & Long, J. H. (2010). Flapping flexible fish: periodic and secular body reconfigurations in swimming lamprey, *Petromyzon marinus*. In *Animal Locomotion* (eds G. Taylor, M. S. Triantafyllou and C. Tropea), pp. 141–159. Springer, Berlin.
Rosen, M. W. (1959). *Water Flow about a Swimming Fish*, pp. 1–96. US Naval Ordnance Test Station, China Lake, CA.
Ryczko, D., Knüsel, J., Crespi, A., Lamarque, S., Mathou, A., Ijspeert, A. J. & Cabelguen, J. M. (2015). Flexibility of the axial central pattern generator network for locomotion in the salamander. *Journal of Neurophysiology* **113**, 1921–1940.
Salazar, R., Fuentes, V. & Abdelkefi, A. (2018). Classification of biological and bioinspired aquatic systems: a review. *Ocean Engineering* **148**, 75–114.

Sánchez-Rodríguez, J., Raufaste, C. & Argentina, M. (2023). Scaling the tail beat frequency and swimming speed in underwater undulatory swimming. *Nature Communications* **14**, 5569.

Satterfield, D. R., Claverie, T. & Wainwright, P. C. (2023). Body shape and mode of propulsion do not constrain routine swimming in coral reef fishes. *Functional Ecology* **37**, 343–357.

Schanz, D., Gesemann, S. & Schröder, A. (2016). Shake-The-Box: Lagrangian particle tracking at high particle image densities. *Experiments in Fluids* **57**, 1–27.

Segall, M., Cornette, R., Fabre, A. C., Godoy-Diana, R. & Herrel, A. (2016). Does aquatic foraging impact head shape evolution in snakes? *Proceedings of the Royal Society B: Biological Sciences* **283**, 20161645.

Seo, E., Yoon, G. Y., Kim, H. N., Lim, J. H., Kim, S., Kim, B., Kim, K. H. & Lee, S. J. (2020). Morphological features of mucous secretory organ and mucous secretion of loach *Misgurnus anguillicaudatus* skin for friction drag reduction. *Journal of Fish Biology* **96**, 83–91.

Sfakiotakis, M., Lane, D. M. & Davies, J. (1999). Review of fish swimming modes for aquatic locomotion. *IEEE Journal of Oceanic Engineering* **24**, 237–252.

Shadwick, R. E. & Gemballa, S. (2005). Structure, kinematics, and muscle dynamics in undulatory swimming. In *Fish Physiology: Fish Biomechanics* (Volume **23**), pp. 241–280. Elsevier Academic Press, London.

Shadwick, R. E. & Lauder, G. V. (2005). *Fish Physiology: Fish Biomechanics*. Elsevier Academic Press, London.

Shepard, D. (1968). A two-dimensional interpolation function for irregularly-spaced data. In *Proceedings of the 1968 23rd ACM national conference*, pp. 517–524. Association for Computing Machinery, New York.

Smits, A. J. (2019). Undulatory and oscillatory swimming. *Journal of Fluid Mechanics* **874**, 1.

Stamhuis, E. J. & Videler, J. J. (1995). Quantitative flow analysis around aquatic animals using laser sheet particle image velocimetry. *Journal of Experimental Biology* **198**, 283–294.

Stin, V., Godoy-Diana, R., Bonnet, X. & Herrel, A. (2023). Measuring the 3D wake of swimming snakes (*Natrix tessellata*) using volumetric particle image velocimetry. *Journal of Experimental Biology* **226**, jeb245929.

Tack, N. B., Du Clos, K. T. & Gemmell, B. J. (2021). Anguilliform locomotion across a natural range of swimming speeds. *Fluids* **6**, 127.

Taylor, G. (1952). Analysis of the swimming of long and narrow animals. *Proceedings of the Royal Society of London. Series A Mathematical and Physical Sciences* **214**, 158–183.

Taylor, G., Triantafyllou, M. S. & Tropea, C. (2010). *Animal Locomotion*. Springer Science & Business Media, Berlin.

Taylor, G. K., Nudds, R. L. & Thomas, A. L. (2003). Flying and swimming animals cruise at a Strouhal number tuned for high power efficiency. *Nature* **425**, 707–711.

Thandiackal, R., Melo, K., Paez, L., Herault, J., Kano, T., Akiyama, K., Boyer, F., Ryczko, D., Ishiguro, A. & Ijspeert, A. J. (2021). Emergence of robust self-organized undulatory swimming based on local hydrodynamic force sensing. *Science Robotics* **6**, eabf6354.

Tokíc, G. & Yue, D. K. (2012). Optimal shape and motion of undulatory swimming organisms. *Proceedings of the Royal Society B: Biological Sciences* **279**, 3065–3074.

Tokíc, G. & Yue, D. K. (2019). Energetics of optimal undulatory swimming organisms. *PLoS Computational Biology* **15**, e1007387.

Triantafyllou, G. S., Triantafyllou, M. S. & Grosenbaugh, M. A. (1993). Optimal thrust development in oscillating foils with application to fish propulsion. *Journal of Fluids and Structures* **7**, 205–224.

Triantafyllou, M. S., Triantafyllou, G. S. & Yue, D. K. (2000). Hydrodynamics of fishlike swimming. *Annual Review of Fluid Mechanics* **32**, 33–53.

Tu, H., Wang, F., Wang, H., Gao, Q. & Wei, R. (2022). Experimental study on wake flows of a live fish with time-resolved tomographic PIV and pressure reconstruction. *Experiments in Fluids* **63**, 1–12.

Tytell, E. D. (2004*a*). Kinematics and hydrodynamics of linear acceleration in eels, *Anguilla rostrata*. *Proceedings of the Royal Society of London. Series B: Biological Sciences* **271**, 2535–2540.

Tytell, E. D. (2004*b*). The hydrodynamics of eel swimming II. Effect of swimming speed. *Journal of Experimental Biology* **207**, 3265–3279.

Tytell, E. D., Borazjani, I., Sotiropoulos, F., Baker, T. V., Anderson, E. J. & Lauder, G. V. (2010*a*). Disentangling the functional roles of morphology and motion in the swimming of fish. *Integrative and Comparative Biology* **50**, 1140–1154.

Tytell, E. D., Carr, J. A., Danos, N., Wagenbach, C., Sullivan, C. M., Kiemel, T., Cowan, N. J. & Ankarali, M. M. (2018). Body stiffness and damping depend sensitively on the timing of muscle activation in lampreys. *Integrative and Comparative Biology* **58**, 860–873.

Tytell, E. D., Cooper, L. O., Lin, Y. L. & Reis, P. M. (2023). Regulation of the swimming kinematics of lampreys *Petromyzon marinus* across changes in viscosity. *Journal of Experimental Biology* **226**, jeb245457.

Tytell, E. D., Holmes, P. & Cohen, A. H. (2011). Spikes alone do not behavior make: why neuroscience needs biomechanics. *Current Opinion in Neurobiology* **21**, 816–822.

Tytell, E. D., Hsu, C. Y., Williams, T. L., Cohen, A. H. & Fauci, L. J. (2010*b*). Interactions between internal forces, body stiffness, and fluid environment in a neuromechanical model of lamprey swimming. *Proceedings of the National Academy of Sciences* **107**, 19832–19837.

Tytell, E. D. & Lauder, G. V. (2004). The hydrodynamics of eel swimming: I. Wake structure. *Journal of Experimental Biology* **207**, 1825–1841.

Van Ginneken, V., Antonissen, E., Müller, U. K., Booms, R., Eding, E., Verreth, J. & Van Den Thillart, G. (2005). Eel migration to the Sargasso: remarkably high swimming efficiency and low energy costs. *Journal of Experimental Biology* **208**, 1329–1335.

Van Rees, W. M., Gazzola, M. & Koumoutsakos, P. (2013). Optimal shapes for anguilliform swimmers at intermediate Reynolds numbers. *Journal of Fluid Mechanics* **722**, R3.

Van Rees, W. M., Gazzola, M. & Koumoutsakos, P. (2015). Optimal morphokinematics for undulatory swimmers at intermediate Reynolds numbers. *Journal of Fluid Mechanics* **775**, 178–188.

Van Weerden, J. F., Reid, D. A. & Hemelrijk, C. K. (2014). A meta-analysis of steady undulatory swimming. *Fish and Fisheries* **15**, 397–409.

Vandenberghe, N., Zhang, J. & Childress, S. (2004). Symmetry breaking leads to forward flapping flight. *Journal of Fluid Mechanics* **506**, 147–155.

Videler, J., Müller, U. & Stamhuis, E. (1999). Aquatic vertebrate locomotion: wakes from body waves. *Journal of Experimental Biology* **202**, 3423–3430.

Videler, J. J. (1993). *Fish Swimming*, Edition (Volume **10**), pp. 1–260. Springer Science & Business Media, London.

Wainwright, D. K. & Lauder, G. V. (2017). Mucus matters: the slippery and complex surfaces of fish. In *Functional Surfaces in Biology III: Diversity of the Physical Phenomena* (eds S. N. Gorb and E. V. Gorb), pp. 223–246. Springer, Cham.

Ward, A. B. & Mehta, R. S. (2010). Axial elongation in fishes: using morphological approaches to elucidate developmental mechanisms in studying body shape. *Integrative and Comparative Biology* **50**, 1106–1119.

Wardle, C., Videler, J. & Altringham, J. (1995). Tuning in to fish swimming waves: body form, swimming mode and muscle function. *Journal of Experimental Biology* **198**, 1629–1636.

Webb, P. W. (1971). The swimming energetics of trout: II. Oxygen consumption and swimming efficiency. *Journal of Experimental Biology* **55**, 521–540.

Webb, P. W. (1975). Hydrodynamics and energetics of fish propulsion. *Bulletin–Fisheries Research Board of Canada* **190**, 1–158.

Webb, P. W. (1984). Form and function in fish swimming. *Scientific American* **251**, 72–83.

Webb, P. W., Hardy, D. H. & Mehl, V. L. (1992). The effect of armored skin on the swimming of longnose gar, *Lepisosteus osseus*. *Canadian Journal of Zoology* **70**, 1173–1179.

Webb, P. W., Kostecki, P. T. & Stevens, E. D. (1984). The effect of size and swimming speed on locomotor kinematics of rainbow trout. *Journal of Experimental Biology* **109**, 77–95.

Webb, P. W. & Weihs, D. (1986). Functional locomotor morphology of early life history stages of fishes. *Transactions of the American Fisheries Society* **115**, 115–127.

Wen, L., Weaver, J. C., Thornycroft, P. J. & Lauder, G. V. (2015). Hydrodynamic function of biomimetic shark skin: effect of denticle pattern and spacing. *Bioinspiration & Biomimetics* **10**, 066010.

Wilga, C. A. & Lauder, G. V. (2004). Biomechanics of locomotion in sharks, rays, and chimeras. In *Biology of Sharks and Their Relatives* (Volume **5**), pp. 139–164. CRC Press, Boca Raton, FL.

Williams, T. L., Grillner, S., Smoljaninov, V. V., Wallén, P., Kashin, S. & Rossignol, S. (1989). Locomotion in lamprey and trout: the relative timing of activation and movement. *Journal of Experimental Biology* **143**, 559.

Williams, T. L. & McMillen, T. (2015). Strategies for swimming: explorations of the behaviour of a neuro-musculo-mechanical model of the lamprey. *Biology Open* **4**, 253–258.

Wu, T. Y. (1961). Swimming of a waving plate. *Journal of Fluid Mechanics* **10**, 321–344.

Wu, T. Y. (1971). Hydromechanics of swimming propulsion. Part 3. Swimming and optimum movements of slender fish with side fins. *Journal of Fluid Mechanics* **46**, 545–568.

Wu, T. Y. (2011). Fish swimming and bird/insect flight. *Annual Review of Fluid Mechanics* **43**, 25–58.

Yanase, K. & Saarenrinne, P. (2015). Unsteady turbulent boundary layers in swimming rainbow trout. *Journal of Experimental Biology* **218**, 1373–1385.

(*Received 19 January 2024; revised 18 June 2024; accepted 19 June 2024*)